

I-C METHANOL SYNTHESIS PROCESS

by

Sadettin S. Ozturk

and

Yatish T. Shah

Chemical and Petroleum Engineering Department
University of Pittsburgh
Pittsburgh, PA 15261

CONTENTS

<u>Section</u>	<u>Page</u>
I-C	METHANOL SYNTHESIS PROCESS
	SUMMARY..... I-172
	Introduction..... I-173
	Model Description..... I-178
	Fixed-Bed Reactor Design for Methanol Synthesis..... I-180
	Parameter Effect on Reactor Performance..... I-195
	Slurry-Bed Reactor Design for Methanol Synthesis..... I-210
	Parameter Effect on Reactor Performance..... I-221
	Comparison of the Performances of Fixed and Bubble Column Reactors for Methanol Synthesis..... I-239
	Parameter Estimation for Fixed-Bed Reactor..... I-243
	Parameter Estimation for Slurry-Bed Reactor..... I-260
	Nomenclature..... I-265
	References..... I-268
	Appendix I-C..... I-C-1

LIST OF FIGURES

	<u>Page</u>
I-C-1	Conventional Coal Based ICI's Methanol Process..... I-176
I-C-2	ICI's Quench Type Reactor..... I-177
I-C-3	Concentration Profiles Along the Pellet Radius..... I-197
I-C-4	Temperature and Concentration Profiles in a Fixed Bed Methanol Synthesis Reactor..... I-198
I-C-5	Effectiveness Factors and Effective Reaction Rates for Methanol Synthesis and Shift Reaction..... I-199
I-C-6	Conversion and Dimensionless Temperature Profiles for a Fixed Bed Methanol Synthesis Reactor..... I-201
I-C-7	Space Time Yield in Fixed Bed Methanol Synthesis Reactor..... I-202
I-C-8	Effect of Gas Velocity on Temperature and Conversion.... I-203
I-C-9	Effect of Gas Velocity on STY..... I-204
I-C-10	Effect of Pressure on Conversion..... I-205
I-C-11	Effect of Pressure on STY..... I-206
I-C-12	Effect of Feed Temperature on Conversion..... I-208
I-C-13	Effect of Feed Temperature on STY..... I-209
I-C-14	Liquid Phase Methanol Synthesis Process..... I-212
I-C-15	Concentration Profiles in a Bubble Column Slurry Reactor..... I-222
I-C-16	Conversion Profile in a Bubble Column Slurry Reactor.... I-223
I-C-17	Temperature and Catalyst Concentration Profile..... I-225
I-C-18	Effect of Column Diameter on Conversion..... I-226
I-C-19	Effect of Column Diameter on STY..... I-227
I-C-20	Effect of Column Height on Conversion..... I-228
I-C-21	Effect of Column Height on STY..... I-229
I-C-22	Effect of Slurry Velocity on Conversion..... I-230

LIST OF FIGURES (Continued)

	<u>Page</u>
I-C-23 Effect of Slurry Velocity on STY.....	I-231
I-C-24 Effect of Gas Velocity and Catalyst Loading on Conversion.....	I-233
I-C-25 Effect of Gas Velocity and Catalyst Loading on STY.....	I-234
I-C-26 Effect of Temperature on Conversion.....	I-235
I-C-27 Effect of Temperature on STY.....	I-236
I-C-28 Effect of Pressure on Conversion.....	I-237
I-C-29 Effect of Pressure on STY.....	I-238
I-C-30 Comparison of Fixed and Slurry Bed Reactors.....	I-240
I-C-31 Comparison of Fixed and Slurry Bed Reactors.....	I-241

LIST OF TABLES

	<u>Page</u>
I-C-1 Syngas Composition Used in Methanol Synthesis.....	I-175

SUMMARY

The synthesis of methanol from CO and H₂ has conventionally been carried out in a fixed bed reactor in the gas phase. Recently, liquid phase methanol synthesis in a slurry reactor has received considerable attention due to the advantages of easy temperature control and the absence of diffusional resistances. In this report, the reactors used for gas phase and liquid phase methanol synthesis are analyzed. The fixed bed reactor is modeled using a one dimensional heterogeneous model while the slurry bed reactor is modeled using a plug flow model for the gas phase and the axial dispersion model for the slurry phase. The physical and thermodynamic properties of the systems are estimated by literature correlations. The main assumptions underlying the model equations are stated and solution techniques described. For each type of reactor, the effects of various parameters such as temperature, pressure, phase velocities, diameter and height of reactor are investigated with the help of the developed simulators. Finally, a comparison of the reactors is presented.

Introduction

Methanol is a basic industrial chemical that is produced at an annual rate of over ten millions tons. Plant capacity for methanol is increasing and there is the possibility that its use, chiefly as a fuel, will eventually require large additional amounts of methanol (Brainard et al., 1984).

There are many reasons why methanol is an important key to a syngas based fuels and chemical industry. First, methanol is synthesized in over 99% or greater selectivity, in sharp contrast to the melange of products, from methane to waxes, obtained in the F-T reaction. Second, the weight retention of syngas ($2H_2:1CO$) as a feedstock for methanol is 100%. Syngas is a costly raw material for the production of the hydrocarbons obtained in the F-T reaction where oxygen is eliminated as water or CO_2 . Third, methanol furnishes selective pathways to a number of important chemicals, including formaldehyde and the widely used two carbon oxygenated chemicals. This route to fuels and to two carbon chemicals from methanol is presently more attractive than their direct synthesis from syngas.

In addition to the many uses of this versatile compound, chiefly as a fuel, there is the exciting discovery that methanol can be converted to high octane gasoline by Mobil's methanol to gasoline (MTG) process using a shape selective zeolite (ZSM-5) catalyst (Chang, 1983). A plant which will produce some 14,000 barrels per day of high octane gasoline from methanol will go on stream in New Zealand in 1985. The MTG process has been discussed in this report (Part I.A).

Traditionally, methanol has been produced by catalytic hydrogenation of carbon monoxide:





Although, several side reactions can take place, the following two are of importance:



All these reactions are reversible and only two of them are independent. For the main reaction (reaction 1), the conversion achievable is greatly limited by thermodynamic equilibrium and since the reaction is exothermic and involves a contraction in volume, highest yields and conversions of methanol are obtained at high pressures and low temperatures. Several generations of catalysts have been developed to get a reasonable reaction rate. Zinc chromium oxide was one of the earliest used. Later a catalyst based on a mixed zinc, copper oxide supported on chromium oxide or aluminum oxide was introduced. Due to the necessity of having the catalyst at desired activity, high temperatures are needed and therefore high pressures are used to enhance the thermodynamically limited yield (high pressure synthesis). It is apparent that an active low-temperature catalyst is highly desirable because the yield would not be limited by thermodynamic equilibrium and the requirement of high pressure could be reduced (Kung, 1980).

In 1966, ICI introduced their low pressure methanol process in low tonnage plants, taking advantage of a much more active catalyst. Initially, the process was only a little more expensive than the high pressure process it replaced, but growing experience in the technology has led to considerable

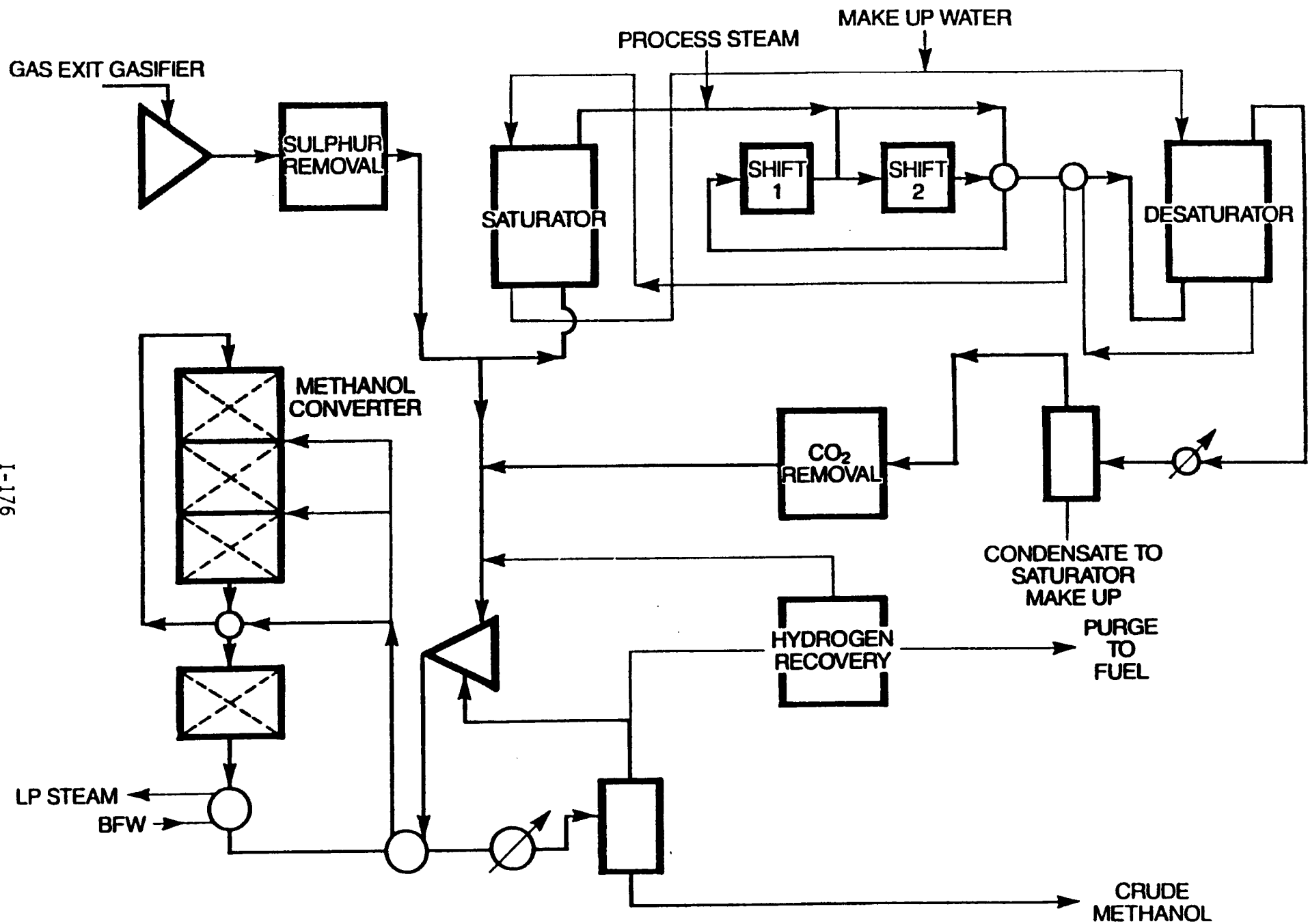
reduced costs and lower energy consumption per ton of product. Now it is used worldwide, and accounts for about 75% of methanol production (Macnaughton et al., 1984).

In the conventional coal based process (Figure I-C-1) the synthesis gas is first passed over a shift catalyst before or after sulphur removal to give a gas composition close to the stoichiometric requirement. The composition of syngas before and after the shift is given in Table I-C-1, for Texaco gasification.

Table I-C-1: Syngas Composition Used in Methanol Synthesis

	Texaco		Lurgi
	Unbalanced Gas Mole %	Balanced Gas Mole %	Gasifier Type Mole %
H ₂	35	55	50
CO	51	19	25
CO ₂	13	5	10
Inerts	1	21	15
H ₂ /CO ratio	0.69	2.89	2.00
Balance Ratio H ₂ /(CO+1.5CO ₂)	0.50	2.08	1.25

The ICI low-pressure process utilizes a single bed of catalyst and quench cooling by "lozenge" distributors especially designed to obtain good gas distribution and gas mixing and to permit rapid loading and unloading of catalyst. A schematic diagram of such a reactor is shown in Figure I-C-2. A low-pressure methanol synthesis process is advantageously combined with production of syngas by partial oxidation since the latter can be carried out



I-176

Figure I-C-1: Conventional coal based ICI's methanol process (Macnaughton et al. 1984)

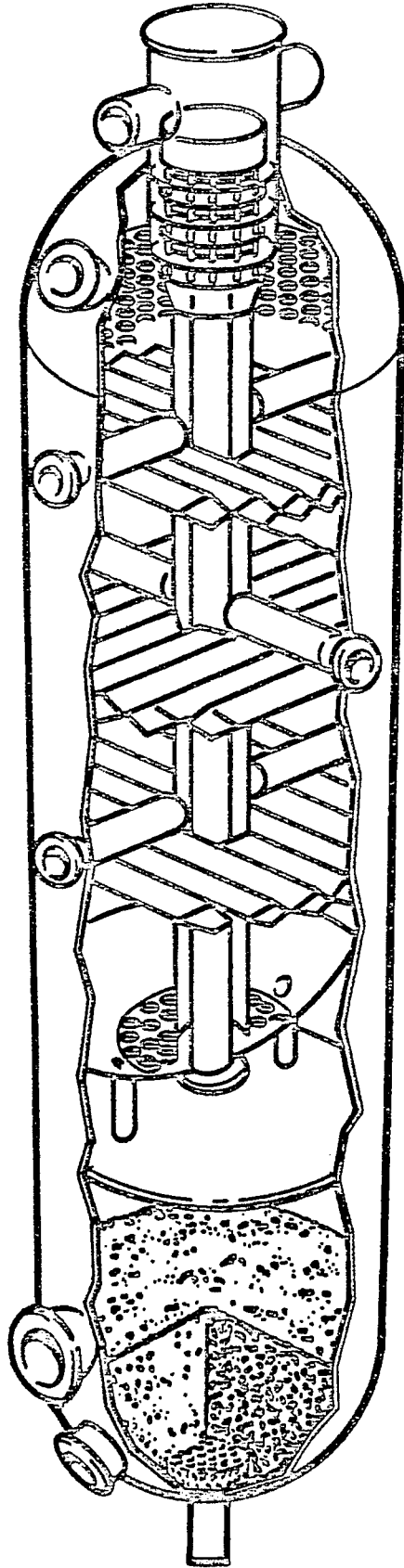


Figure I-C-2: ICI's quench type reactor (Macnaughton et al. 1984)

at methanol synthesis pressure, thus avoiding the necessity of intermediate gas compression. Typical operating conditions for the process are: pressure, 5 to 10 MPa and temperature from 220 to 260°C. The reactor operates adiabatically and temperature rise at each bed is known to be extremely high. The overall effectiveness factor is less than 0.5.

Liquid phase methanol process (LPMeOH) was recently evaluated against the conventional multibed quench system (Sherwin and Frank, 1976). Various projects sponsored by EPRI at Chem-Systems and Air Products and Chemical Co., on the three phase synthesis clarified some of the important economic factors (Sherwin and Blum, 1979; Bonnell and Weimer, 1984). Here, syngas containing CO, CO₂ and H₂ is passed upward into the bubble column slurry reactor concurrent with the inert hydrocarbon (Witco-40 or Freezene-100) which serves to both fluidize the catalyst and absorb the exothermic heat of reaction. Due to the easy temperature control and the absence of diffusional resistances, this type of reactor has received considerable attention.

In this part of the project, both gas phase and liquid phase methanol synthesis are analyzed. Computer programs for the simulation of fixed and slurry bed methanol synthesis reactors have been developed to make a comparison between these two type of operations. Model equations are derived and the solution techniques are included in this report. A case study has been analyzed and the results of the simulations are compared with a discussion on the reactor performance.

Model Description

This part includes the model developments for fixed and slurry bed low-pressure methanol synthesis reactors, and descriptions of the mathematical procedures to predict the performance of the units. Due to the distinct differences in the design and operation of these two reactor systems, analyses

are presented separately. The physical and thermodynamic properties of the systems (gas and liquid phase reactor system) are estimated by correlations and these methods are also included in this part of the report. The main assumptions underlying the model equations are stated and solution techniques for final form of the equations are described. For each type of reactor, the effects of various parameters on the performance are investigated with the help of simulators developed. Finally a comparison of the reactors is presented.

Fixed-Bed Reactor Design for Methanol Synthesis

Fixed-bed reactor is the traditional reactor type to carry out the methanol synthesis reaction. It refers to two-phase systems in which the reacting gas flows through a bed of catalyst particles or pellets (Froment and Bischoff, 1979).

Two-phase boundaries inherent in fixed-bed reactors require that transport processes (mass and energy transfer) as well as the intrinsic reaction rate be accounted in reactor design. The model equations should include transport restrictions against mass and heat transfer in the interior and in the gas film surrounding the particle.

For a catalytic reaction taking place in a fixed-bed reactor, because of the resistance against mass transport through the gas film, a concentration gradient is required so that the concentration of reactants is lower on the particle surface than in bulk phase. If the reaction is exothermic, the heat produced must be transported away and this requires a temperature gradient. The resistances for these two transport processes are called external resistances and they can be very severe depending on the conditions. On the other hand, the concentrations and the temperature at the catalyst surface cannot have the same value throughout a porous catalyst particle due to mass and energy transport restrictions. These last mentioned effects are called internal resistances. The combined effect of internal and external resistances is that the concentrations of the reactants in the interior of the particle will be lower than for bulk phase and for an exothermic reaction the temperature will be higher than the bulk gas temperature. As the reaction rate is affected by concentrations and temperature, the intrinsic rate cannot directly be used with the bulk concentrations and temperature.

The mathematical model which allows for differences in concentrations and temperature between the bulk gas stream and the particles is called the heterogeneous reactor model (Froment, 1974). This is contrary to the so called pseudo-homogeneous model for a catalytic reactor, where the concentrations and temperature in the bulk gas phase and in the particles are considered identical. Since the concentrations of the reactant gases are always lowered by the internal and external mass transfer resistances and the temperature at the catalyst site differs from the bulk temperature, the last mentioned model is known to be less appropriate and should be avoided in most cases.

In the heterogeneous reactor model, the effects of the internal and external resistances on the reaction rate are accounted by using global or overall rather than intrinsic rates. These type of rates are expressed in terms of gas phase conditions and they can directly be used in the axial integration of mass and energy balance differential equations.

The overall effectiveness factor is now introduced as a quantitative measure of the combined effects of transport restrictions. It is defined as the ratio of the average rate of reaction, which would have been obtained, if there had been no transport resistance, i.e. as if the temperature and gas composition had been the same inside the particle as in the bulk gas phase. Once this factor is known, the overall rate can easily be obtained by multiplying it with the rate evaluated at bulk conditions. The calculation of such a factor involves a solution of solid phase differential mass and energy balance equations with appropriate boundary conditions. In this procedure, the internal resistances are accounted by differential equation itself, and the effect of external resistances are imposed by boundary conditions.

Due to the complex nature of the rate expressions, the presence of two reactions (reaction 1 and 2) and the large heat effects, the overall effectiveness factor calculation for methanol synthesis is not an easy matter. Early studies on the modeling of methanol synthesis reactors are therefore limited to the degree of sophistication on the evaluation of these factors. For instance, in the work by Cappelli et al., only reaction 1 is considered and temperature effects are neglected (Cappelli et al. 1972).

So far, only two works have been presented in the literature for the simulation of fixed-bed methanol synthesis reactors (Cappelli et al., 1972; Bakemeier, 1970). Since they both are for high pressure catalyst, their results cannot be applied to low pressure synthesis where Cu-based catalyst is used. In the present work, a simulator program has been developed for the design and simulation of methanol synthesis reactors. The simulator is designed to be capable of handling different catalysts and can be used for both types of synthesis. A general procedure of effectiveness factor calculations for a single catalyst particle in which several chemical reactions can take place is presented.

a. Model Assumptions

In the model development, the following arguments are made:

i) The significance of axial dispersion depends on the reactor length, the effective diffusivity and the gas velocity. For high velocities ($Re > 1$) and for the reactors where length to diameter ratio is well above unity, axial dispersion is negligible. Therefore a plug flow model will be used.

ii) Since radial gradients in concentration and temperature are caused solely by radial variation in axial velocity and since in plug-flow case, the axial velocity is only dependent on the axial direction, radial profiles can be neglected in an adiabatic plug flow reactor. Therefore, one-dimensional model will be used to be a good representation of actual behavior.

iii) Unlike high pressure synthesis, the low pressure synthesis operates at relatively moderate pressure and temperatures where the nonideality of the gas mixture can be neglected. The rate expressions for low pressure synthesis are also based on the concentrations rather than fugacities, suggesting that the ideal gas law can be applicable. In the model equations ideal gas law will be used but for the rate expressions based on the fugacities, the nonideality will be considered.

iv) The presence of two simultaneous reactions with very nonlinear rate equations makes the use of the Stefan-Maxwell equation for the mixture gas diffusivities difficult. Hence Wilke's equation will be used to calculate the diffusivities in gas mixture.

In this work, we wish to present a model as general as possible. Therefore, the following points which were neglected by other studies will be considered:

i) Both reactions, methanol formation and shift reaction proceed with finite reaction rates and neither of them is considered at equilibrium.

ii) The temperature gradients inside the pellets can be very important. Hence nonisothermal effectiveness factors should be calculated with the solution of solid phase balances.

iii) Since the total number of moles change due to reaction 1, the concentration profiles would be affected. This effect is accounted in gas phase material balances, but since it leads to a more complicated problem in the calculation of effective reaction rates it was assumed negligible in the solid phase.

iv) Physical properties are considered as a function of temperature and pressure. Gas velocity will also change in the axial direction (due to temperature and total number of moles variations) leading to variable heat and mass transfer parameters and also mixture properties along the reactor length.

b. Model Equations

Based on the above conclusions, the following model equations can be written. In these equations methanol and CO₂ are chosen as key components and the first two reactions (1 and 2) are considered independent reactions.

1. Mass Balances:

(a) Gas Phase

i. Methanol

$$\frac{d}{dx} (U C_M^g) = (k_g)_M a_v ((C_M^s)_{r=R} - C_M^g) \quad (4)$$

ii. CO₂

$$\frac{d}{dx} (U C_{CO_2}^g) = (k_g)_{CO_2} a_v ((C_{CO_2}^s)_{r=R} - C_{CO_2}^g) \quad (5)$$

(b) Solid Balance

i. Methanol

$$\frac{(D_M) e}{r^2} \frac{d}{dr} \left(r^2 \frac{dC_M^s}{dr} \right) = r_1 \rho_p \quad (6)$$

ii. CO₂

$$\frac{(D_{CO_2})}{r^2} e \frac{d}{dr} \left(r^2 \frac{dC_{CO_2}^s}{dr} \right) = -r_2 \rho_p \quad (7)$$

Here effective diffusivities are assumed constant and evaluated at bulk gas phase conditions.

2. Energy Balances:

(a) Gas Phase

$$\frac{d}{dx} (U \rho C_p T^g) = h a_v ((T^s)_{r=R} - T^g) \quad (8)$$

(b) Solid Phase

$$\frac{\lambda_e}{r^2} \frac{d}{dr} \left(r^2 \frac{dT^s}{dr} \right) = ((-\Delta H_R)_1 r_1 + (-\Delta H_R)_2 r_2) \rho_p \quad (9)$$

Boundary Conditions:

$$@ z = 0 \quad C_1^g = C_{i,o}^g \quad T^g = T_o^g, \quad U = U_o \quad (10)$$

$$@ r = 0 \quad \frac{dC_M^s}{dr} = \frac{dC_{CO_2}^s}{dr} = \frac{dT^s}{dr} = 0 \quad (11)$$

$$@ r = R \quad (k_g)_M ((C_M^s)_{r=R} - C_M^g) = -(D_M)_e \left(\frac{dC_M^s}{dr} \right)_{r=R}$$

$$(k_g)_{CO_2} ((C_{CO_2}^s)_{r=R} - C_{CO_2}^g) = -(D_{CO_2})_e \left(\frac{dC_{CO_2}^s}{dr} \right)_{r=R} \quad (12)$$

$$h ((T^s)_{r=R} - T^g) = -\lambda_e \left(\frac{dT^s}{dr} \right)_{r=R}$$

c. Solution Technique

By solution of solid phase mass and energy equations (6, 7 and 9) subject to boundary conditions of (11) and (12) we can evaluate effective reaction rates and effectiveness factors:

$$r_1^e = (k_g)_M a_v ((C_M^s)_{r=R} - C_M^g) = -a_v (D_M)_e \left(\frac{dC_M}{dr} \right)_{r=R} \quad (13)$$

and

$$r_2^e = -(k_g)_{CO_2} a_v ((C_{CO_2}^s)_{r=R} - C_{CO_2}^g) = a_v (D_{CO_2})_e \left(\frac{dC_{CO_2}}{dr} \right)_{r=R} \quad (14)$$

where

$$a_v = \frac{6(1 - \epsilon_B)}{d_p}$$

with the help of effective reaction rates, gas phase mass and energy balances became:

$$\text{eq (4)} \quad \frac{d}{dx} (U C_M^g) = r_1^e \quad (15)$$

$$\text{eq (5)} \quad -\frac{d}{dx} (U C_{CO_2}^g) = r_2^e \quad (16)$$

$$\text{eq (8)} \quad -\frac{d}{dx} (U \rho C_p T^g) = r_1^e (-\Delta H)_1 + r_2^e (-\Delta H)_2 \quad (17)$$

instead of integrating eq. (17) we can combine it with eq. (15) and (16) to give:

$$T^g = \frac{U^o \rho^o C_p^o}{U \rho C_p} T_o^g + \frac{(-\Delta H)_1}{U \rho C_p} (U C_M^g - U^o C_{M,o}^g) + \frac{(-\Delta H)_2}{U \rho C_p} (U C_{CO_2}^g - U C_{CO_2,o}^g) \quad (18)$$

here, it is assumed that reaction enthalpies do not change very much with the reactor length and taken as constant.

Use of conversions

Introducing $F_i = UC_i^g$, superficial molar flow rates, we can define conversions X_1 and X_2 as follows:

$$X_1 = \frac{F_M - F_M^o}{F_{CO}^o}, \quad X_2 = \frac{F_{CO_2}^o - F_{CO_2}^o}{F_{CO}^o} \quad (19)$$

Based on these values concentration of each component as well as gas velocity can be expressed: Concentrations

$$1 \quad CO \quad C_1^g = (1 - X_1 + X_2)\beta \quad (20)$$

$$2 \quad CO_2 \quad C_2^g = (\alpha_1 - X_2)\beta \quad (21)$$

$$3 \quad H_2 \quad C_3^g = (\alpha_2 - 2X_1 - X_2)\beta \quad (22)$$

$$4 \quad CH_3OH \quad C_4^g = (\alpha_3 + X_1)\beta \quad (23)$$

$$5 \quad H_2O \quad C_5^g = (\alpha_4 + X_2)\beta \quad (24)$$

$$6 \quad N_2 \quad C_6^g = \alpha_5 \beta \quad (25)$$

$$7 \quad CH_4 \quad C_7^g = \alpha_6 \beta \quad (26)$$

Gas velocity

$$U = U_o C_{CO}^o / \beta$$

Here pressure is taken constant.

In the above equations:

$$\alpha_1 = y_{CO_2}^o / y_{CO}^o, \quad \alpha_2 = y_{H_2}^o / y_{CO}^o, \quad \alpha_3 = y_{CHOH} / y_{CO}^o$$

$$\alpha_4 = y_{H_2O}^o / y_{CO}^o, \quad \alpha_5 = y_{N_2}^o / y_{CO}^o, \quad \alpha_6 = y_{CH_4}^o / y_{CO}^o \quad (27)$$

$$\beta = C_T y_{CO}^o / (1 - 2 y_{CO}^o X_1)$$

In terms of conversions eqns (15, 16 and 18) can be written in the dimensionless form of

$$\text{eq. (15)} \quad \frac{dX_1}{dz} = \phi_1 \quad (28)$$

$$\text{eq. (16)} \quad \frac{dX_2}{dz} = \phi_2 \quad (29)$$

$$\text{eq. (18)} \quad \theta = \alpha - 1 + \Gamma_1 X_1 + \Gamma_2 X_2 \quad (30)$$

where $\phi_1 = r_1^e L / F_{CO}^o$ (31)

$$\phi_2 = r_2^e L / F_{CO}^o \quad (32)$$

$$z = x/L \quad (33)$$

$$\theta = (T^g - T_o^g) / T_o^g \quad (34)$$

$$\alpha = (U^o C_p^o \rho^o) / (U C_p \rho) \quad (35)$$

$$\Gamma_1 = \frac{(-\Delta H)_1}{U \rho C_p T_o^g} F_{CO}^o \quad (36)$$

$$\Gamma_2 = \frac{(-\Delta H)_2}{U \rho C_p T_o^g} F_{CO}^o \quad (37)$$

It is clear that integration of eq. (28) and (29) can easily be performed providing that the effective reaction rates are calculated. At this point, the solution of solid phase balances comes into the picture.

. Calculation of effective reaction rates and effectiveness factors for methanol synthesis:

In a general case where N components are involved in R reactions, the mass balance for the solid phase is

$$D_i \frac{1}{r^2} \frac{d}{dr} \left(r^2 \frac{dC_i}{dr} \right) = - \sum_k^R v_{ik} r_k \rho_p \quad i = 1, 2, \dots, N \quad (38)$$

and the energy balance

$$\lambda \frac{1}{r^2} \frac{d}{dr} \left(r^2 \frac{dT}{dr} \right) = - \sum_k^R r_k \rho_p (-\Delta H)_k \quad (39)$$

Having key components which involve only one reaction

$$D_k \frac{1}{r^2} \frac{d}{dr} \left(r^2 \frac{dC_k}{dr} \right) = -v_k r_k \rho_p \quad (40)$$

equations (38-40) can be written in dimensionless form of:

$$\text{eq. (38)} \quad \frac{1}{\zeta^2} \frac{d}{d\zeta} \left(\zeta^2 \frac{dC_i}{d\zeta} \right) = - \sum_k^R v_{ik} \frac{R^2}{D_i} r_k \rho_p \quad (41)$$

$$\text{eq. (39)} \quad \frac{1}{\zeta^2} \frac{d}{d\zeta} \left(\zeta^2 \frac{dT}{d\zeta} \right) = - \sum_k^R r_k R^2 \frac{(-\Delta H)_k}{\lambda} \rho_p \quad (42)$$

$$\text{eq. (40)} \quad \frac{1}{\zeta^2} \frac{d}{d\zeta} \left(\zeta^2 \frac{dC_i}{d\zeta} \right) = - v_k \frac{R^2}{D_k} r_k \rho_p \quad (43)$$

Note that the suffixes indicating effective values for D_i and λ are omitted.

The boundary conditions are:

$$\text{@ } \zeta = 0 \text{ (r = 0)} \quad \frac{dC_i}{d\zeta} = 0, \quad \frac{dT}{d\zeta} = 0 \quad (44)$$

$$\text{@ } \zeta = 1 \text{ (r = R)} \quad - \frac{dC_i}{d\zeta} = (Sh)_i (C_i^g - C_i) \quad (45)$$

$$- \frac{dT}{d\zeta} = Nu (T^g - T) \quad (46)$$

where

$$\zeta = r/R, \quad Sh_i = (k_g)_i R/D_i \quad (47)$$

$$Nu = hR/\lambda$$

using eq. (41) and (43)

$$\frac{d}{d\zeta} \left(\zeta^2 \frac{dC_i}{d\zeta} \right) = \sum_k \frac{R}{v_k} \left[\frac{v_{ik}}{v_k} \frac{D_k}{D_i} \frac{d}{d\zeta} \left(\zeta^2 \frac{dC_k}{d\zeta} \right) \right] \quad (48)$$

integration between 0 and ζ and using BC: eq. (44)

$$\frac{dC_i}{d\zeta} = \sum_k \frac{R}{v_k} \frac{v_{ik}}{v_k} \frac{D_k}{D_i} \frac{dC_k}{d\zeta} \quad (49)$$

integration between 1 and ζ

$$C_i - (C_i)_{\zeta=1} = \sum_k \frac{R}{v_k} \frac{v_{ik}}{v_k} \frac{D_k}{D_i} (C_k - (C_k)_{\zeta=1}) \quad (50)$$

Application of BC eq. (46) to eq. (49)

$$C_i^g - (C_i)_{\zeta=1} = \sum_k \frac{R v_{ik}}{v_k} \frac{D_k}{D_i} \frac{(Sh)_k}{(Sh)_i} [C_k^g - (C_k)_{\zeta=1}] \quad (51)$$

eliminate $(C_i)_{\zeta=1}$ between eq. (50) and (51)

$$C_i = C_i^g + \sum_k \frac{R v_{ik}}{v_k} \frac{D_k}{D_i} [C_k - (C_k)_{\zeta=1} - \frac{(Sh)_k}{(Sh)_i} (C_k^g - (C_k)_{\zeta=1})] \quad (52)$$

using conversions defined as

$$x_k = \frac{C_k^g - C_k}{C_i^g} \quad \text{or} \quad C_k = C_k^g - C_i^g x_k$$

$$C_i = C_i^g + \sum_k \frac{R v_{ik}}{v_k} \frac{D_k}{D_i} C_i^g [(x_k)_{\zeta=1} [1 - \frac{(Sh)_k}{(Sh)_i}] - x_k] \quad (53)$$

Hence the concentration of each species is expressed in terms of conversions.

For temperature we can use eq. (41) and (42) to give

$$\frac{dT}{d\zeta} (\zeta^2 \frac{dT}{d\zeta}) = \sum_k \frac{R (-\Delta H)_k}{v_k} \frac{D_k}{\lambda} \frac{d}{d\zeta} (\zeta^2 \frac{dC_k}{d\zeta}) \quad (54)$$

integration between 0 and ζ and using BC: eq. (44)

$$\frac{dT}{d\zeta} = \sum_k \frac{R (-\Delta H)_k}{v_k} \frac{D_k}{\lambda} \frac{dC_k}{d\zeta} \quad (55)$$

integration between 1 and 2

$$T - (T)_{\zeta=1} = \sum_k \frac{R (-\Delta H)_k}{v_k} \frac{D_k}{\lambda} (C_k - (C_k)_{\zeta=1}) \quad (56)$$

Application of BC: eq. (40) to eq. (55)

$$T^g - (T)_{\zeta=1} = \sum_k \frac{R (-\Delta H)_k}{v_k} \frac{D_k}{\lambda} \frac{(Sh)_k}{Nu} (C_k^g - (C_k)_{\zeta=1}) \quad (57)$$

eliminate $(T)_{\zeta=1}$ between eq. (56) and (57)

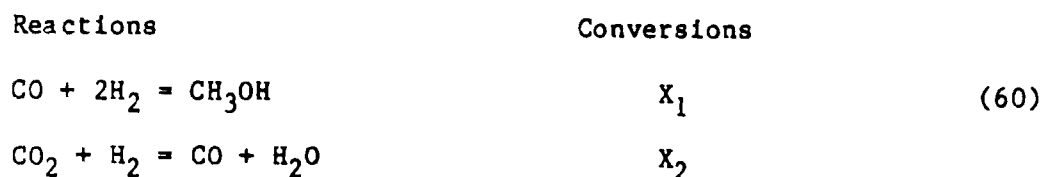
$$T = T^g + \sum_k \frac{R (-\Delta H)_k}{v_k} \frac{D_k}{\lambda} [(C_k - (C_k)_{\zeta=1}) - \frac{(Sh)_k}{Nu} (C_k^g - (C_k)_{\zeta=1})] \quad (58)$$

and using conversions:

$$T = T^g + \sum_k \frac{R (-\Delta H)_k}{v_k} \frac{D_k}{\lambda} C_1^g [(X_k)_{\zeta=1} [1 - \frac{(Sh)_k}{Nu}] - X_k] \quad (59)$$

Hence the problem becomes to evaluate the conversion profiles along the pellet radius. Once the conversions are known the concentration and temperature profiles can be obtained by eq. (53) and (59) respectively.

In methanol synthesis CO_2 and CH_3OH can be chosen as key components



However, to get positive values for X_1 we can put

$$X_1 = \frac{C_{CH_3OH} - C_{CH_3OH}^g}{C_{CO}^g} \quad (61)$$

while the standard definition for X_2 remains the same

$$X_2 = \frac{C_{CO_2}^g - C_{CO_2}}{C_{CO}^g} \quad (62)$$

In terms of X_1 and X_2 concentrations and temperature can be expressed as:

Component

$$1. \text{ CO} \quad C_{\text{CO}} = C_{\text{CO}}^g \left[1 - \frac{D_2}{D_1} (X_2)_{\zeta=1} \left(1 - \left(\frac{D_1}{D_2} \right)^{1/3} \right) - X_2 \right] + \frac{D_4}{D_1} \left[(X_1)_{\zeta=1} \left(1 - \left(\frac{D_1}{D_k} \right)^{1/3} \right) - X_1 \right] \quad (63)$$

$$2. \text{ CO}_2 \quad C_{\text{CO}_2} = C_{\text{CO}_2}^g - C_{\text{CO}}^g X_1 \quad (64)$$

$$3. \text{ H}_2 \quad C_{\text{H}_2} = C_{\text{H}_2}^g + C_{\text{CO}}^g \left\{ 2 \frac{D_4}{D_3} \left[(X_1)_{\zeta=1} \left(1 - \left(\frac{D_3}{D_4} \right)^{1/3} \right) - X_1 \right] + \frac{D_2}{D_3} \left[(X_2)_{\zeta=1} \left(1 - \left(\frac{D_3}{D_2} \right)^{1/3} \right) - X_2 \right] \right\} \quad (65)$$

$$4. \text{ CH}_3\text{OH} \quad C_{\text{CH}_3\text{OH}} = C_{\text{CH}_3\text{OH}}^g + C_{\text{CO}}^g X_2 \quad (66)$$

$$5. \text{ H}_2\text{O} \quad C_{\text{H}_2\text{O}} = C_{\text{H}_2\text{O}}^g - C_{\text{CO}}^g \frac{D_2}{D_5} \left[(X_2)_{\zeta=1} \left(1 - \left(\frac{D_5}{D_2} \right)^{1/3} \right) - X_2 \right] \quad (67)$$

Temperature

$$T = T^g + A \left[(X_1)_{\zeta=1} \left(1 - \frac{(\text{Sh})_1}{\text{Nu}} \right) - X_1 \right] \quad (68)$$

$$+ B \left[(X_2)_{\zeta=1} \left(1 - \frac{(\text{Sh})_2}{\text{Nu}} \right) - X_2 \right]$$

where:

$$A = D_4 \frac{(-\Delta H)_1}{\lambda} C_1^g \quad (69)$$

$$B = D_2 \frac{(-\Delta H)_2}{\lambda} C_1^g \quad (70)$$

in these equations $\frac{(Sh)_k}{(Sh)_1} = \left(\frac{D_1}{D_k}\right)^{1/3}$ is used (see mass transfer coefficients estimation).

Using the above relationships there remain two differential equations to be solved. In dimensionless form

$$\text{eq. (6)} \quad \frac{1}{\zeta^2} \frac{d}{d\zeta} \left(\zeta^2 \frac{dX_1}{d\zeta} \right) = \psi_1 \quad (71)$$

$$\text{eq. (7)} \quad \frac{1}{\zeta^2} \frac{d}{d\zeta} \left(\zeta^2 \frac{dX_2}{d\zeta} \right) = \psi_2 \quad (72)$$

$$\text{where } \psi_1 = R^2 r_1 \rho_p / (D_4 C_1^g) \quad (73)$$

$$\psi_2 = R^2 r_2 \rho_p / (D_2 C_1^g) \quad (74)$$

Boundary conditions

$$\text{@ } \zeta=0 \quad \frac{dX_1}{d\zeta} = \frac{dX_2}{d\zeta} = 0 \quad (75)$$

$$\text{@ } \zeta=1 \quad \frac{dX_1}{d\zeta} = -(Sh)_4 X_1 \quad (76)$$

$$\frac{dX_2}{d\zeta} = (Sh)_1 X_2 \quad (77)$$

The effective rates are calculated as:

$$r_1^e = -a_v D_4 \frac{C_1^g}{R} \frac{dX_1}{d\zeta} \quad (78)$$

$$r_2^e = -a_v D_2 \frac{C_1^g}{R} \frac{dX_2}{d\zeta} \quad (79)$$

where

$$a_v = \frac{6(1-\epsilon_B)}{d_p} \quad (80)$$

and the overall effectiveness factors are evaluated as:

$$\eta_1 = \frac{r_1^e}{r_1 \text{ (at bulk conditions)}} \quad (81)$$

$$\eta_2 = \frac{r_2^e}{r_1 \text{ (at bulk conditions)}} \quad (82)$$

The solution of eqns. (71) and (72) are performed by COLSYS (Ascher et al., 1981) while the integration of eq. (28) and (29) are carried out by a Runge Kutta method.

The program developed calculates the concentration profiles at bulk gas phase and at the particle center. It also predicts the temperature effective reaction rates and overall effectiveness factors profiles in the axial direction. The conversions are evaluated at each point and finally the space time yield, STY in Nm³ gas converted per kg catalyst per hour is computed.

Parameter Effect on Reactor Performance

The effect of operating and design conditions on the reactor performance is studied to test the simulator. The influence of conversion (overall conversion is used) and the Space Time Yield are presented and explained based on theoretical observations.

To present the goodness of the reactor model, the radial concentration profiles inside the pellet, and the concentration and temperature profiles in the reactor is demonstrated in Figures I-C-3, I-C-4 and I-C-5. In the first figure only the mole fractions for CO, H₂ and CH₃OH are given and since temperature rise was found to be very small (~ 1 K) it is not included. It is clear that diffusional limitations are very strong and should play a very important role in the design calculations. Mass and energy transfer resistances, on, the other hand, were found to be negligible since the surface concentrations (mole fractions for H₂, CO and CH₃OH are 0.5, 0.25 and 0 respectively) are equal to bulk values. The effectiveness factors (overall) are 0.87 and 0.43 for methanol and shift reactions respectively.

In Figure I-C-4 several concentration and temperature profiles are shown for a reactor length of 0.8 m that corresponds to the first bed in ICI's quench reactor. For methanol, the solid phase, pellet center concentration is also included. As it is shown in the figure the mole fraction methanol increases in the gas bulk phase while it shows a maxima for solid phase center concentrations. Temperature increases very rapidly and a temperature rise of 186 K is obtained. Actually this figure is prepared for a gas velocity of 0.1 m/s which is very low (normal value is 0.4 m/s) and this temperature rise is not permitted in a commercial reactor.

The effectiveness factor and effective reaction rates are given in Figure I-C-5. The overall effectiveness factor drops to 0.1 for methanol synthesis reaction (Eff 1) while it behaves in a peculiar way for shift reaction (Eff 2); it goes through a maxima. The effective reaction rates increase at first and then decrease with axial coordinate.

The general trends in conversion and Space Time Yield (STY) are presented in the following pages for the effect of various operating and design

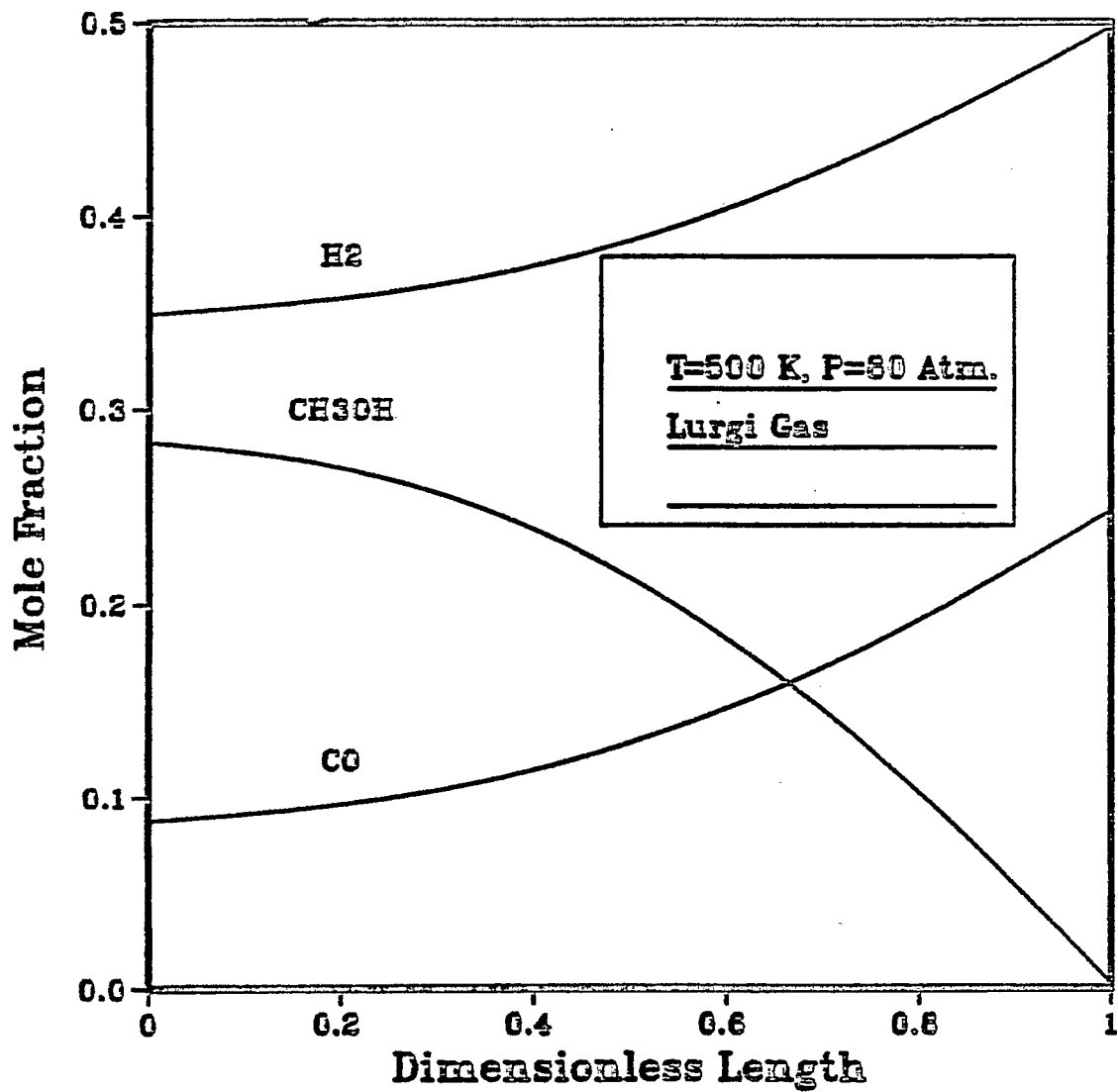


Figure I-C-3: Concentration profiles along the pellet radius

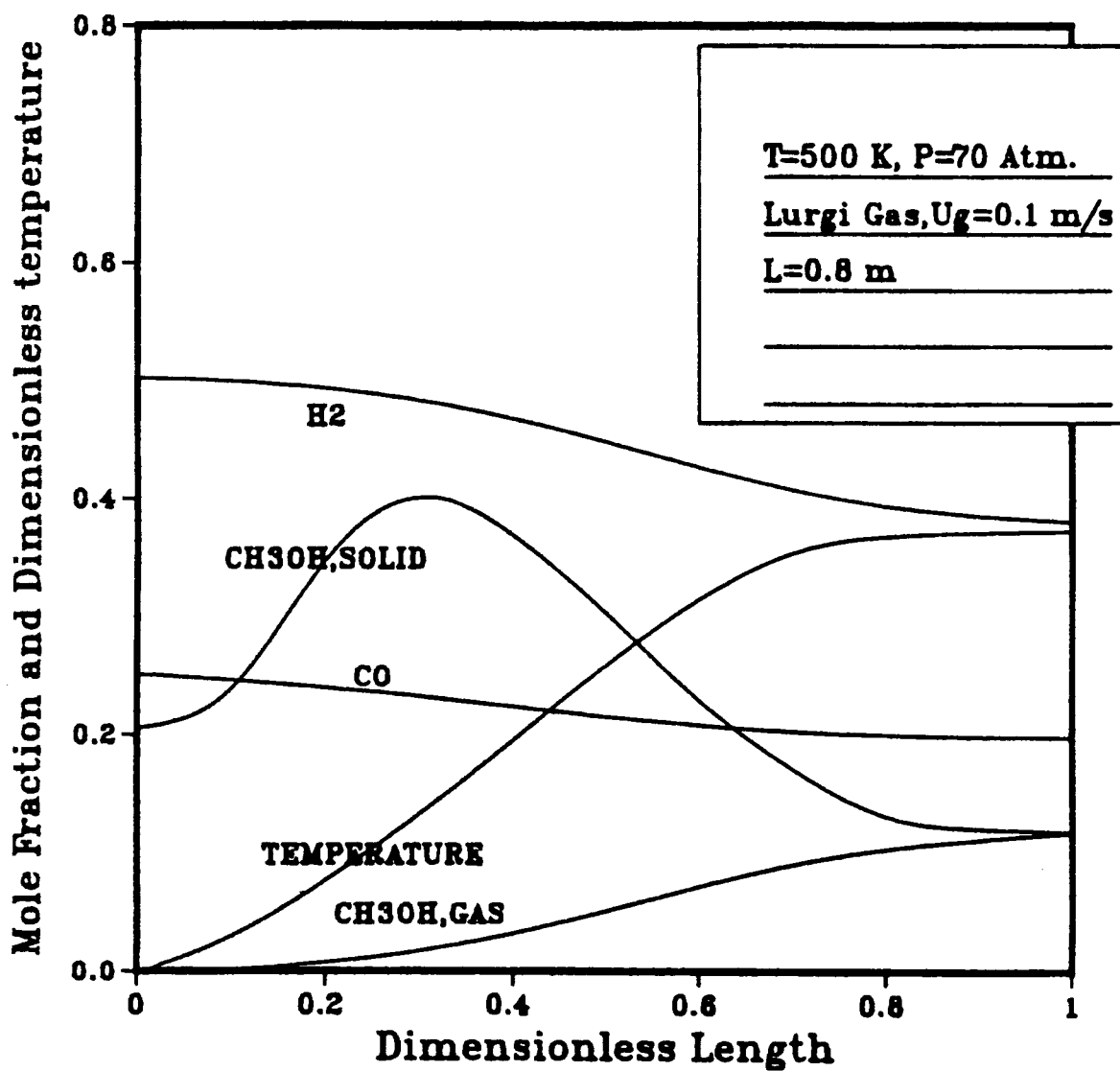


Figure I-C-4: Temperature and concentration profiles in a Fixed Bed Methanol Synthesis Reactor

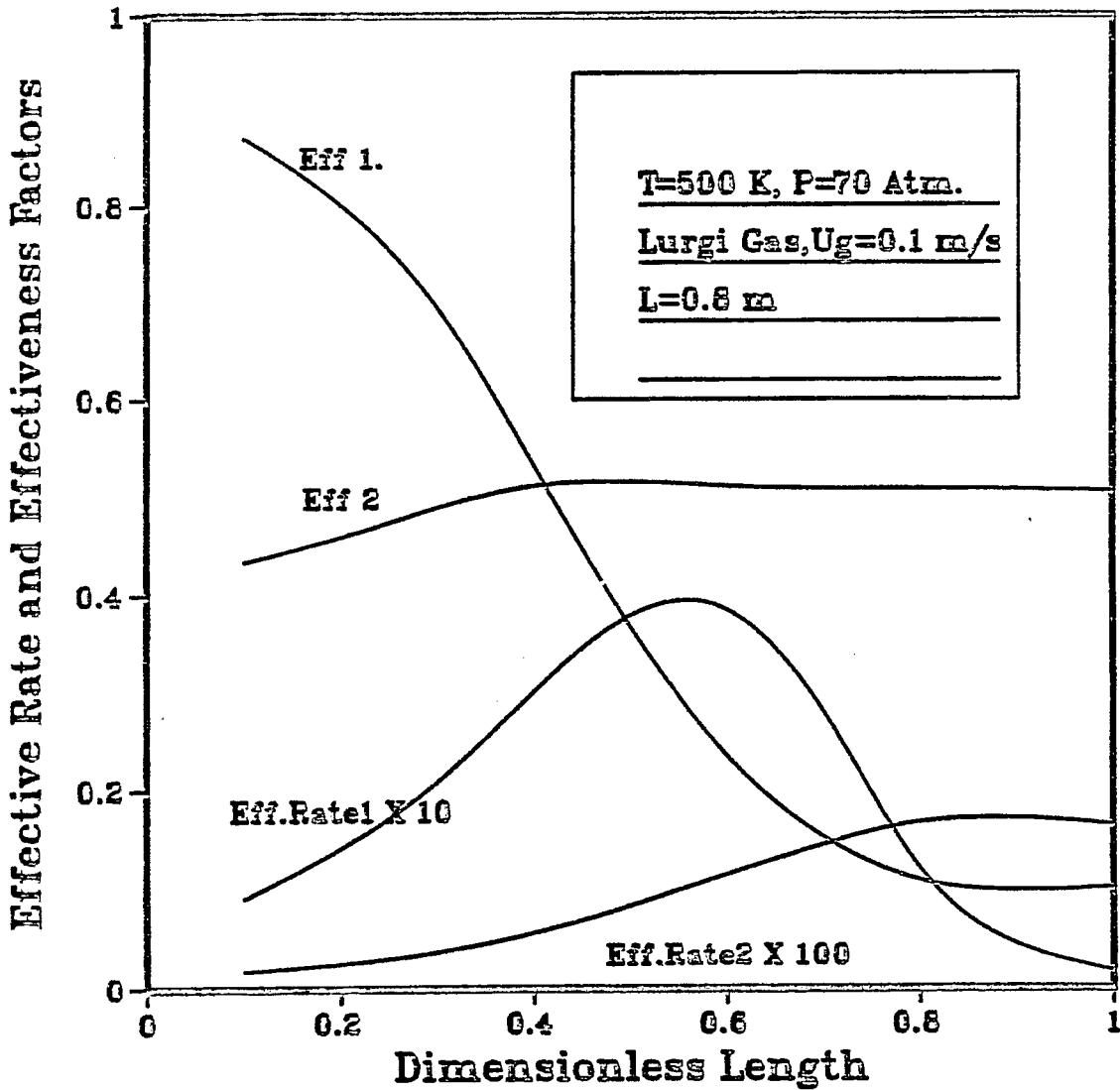


Figure I-C-5: Effectiveness factors and effective reaction rates for methanol synthesis (reaction 1) and shift reaction (reaction 2)

parameters. All the calculations have been made for Lurgi gasifier type syngas composition (Table I-C-1).

a. Effect of Reactor Length

The effect of reactor length on performance was studied at 500 K and 80 atm. A superficial gas velocity of 0.4 m/s is applied. The results are presented in Figure I-C-6 and I-C-7 for conversion and Space Time Yield (STY) respectively. It is apparent that both conversion and STY increase with length to a certain point then equilibrium attains. The outlet temperature is also shown in Figure I-C-6 and it can be seen that the temperature also reaches a limiting value. Obviously for a reactor longer than 2.0 m, no reaction takes place at the top.

b. Effect of Gas Velocity

Increase in the gas velocity leads to a gradual drop in conversion as seen in Figure I-C-8. The Space Time Yield, on the other hand, goes through a maxima (Figure I-C-9). The higher the gas velocity, the lower the residence time and the lower the conversion. However STY directly increases with gas velocity and depends on conversion, leading to such a behavior. The optimum gas velocity under these conditions (500 K, 80 atm and $L = 0.8$ m) can be established as 0.18 m/s.

c. Effect of Pressure

The operating pressure increases both conversion and STY (Figs. I-C-10 and I-C-11) which is not surprising since the concentration of the reactants increases. In the calculations the gas velocity is kept constant at a value of 0.4 m/s. The limit in pressure should be considered in reactor wall material and wall thickness as well as in the cost of compression. The low pressure synthesis operates at a pressure range of 60-100 atm and the same range is used here.

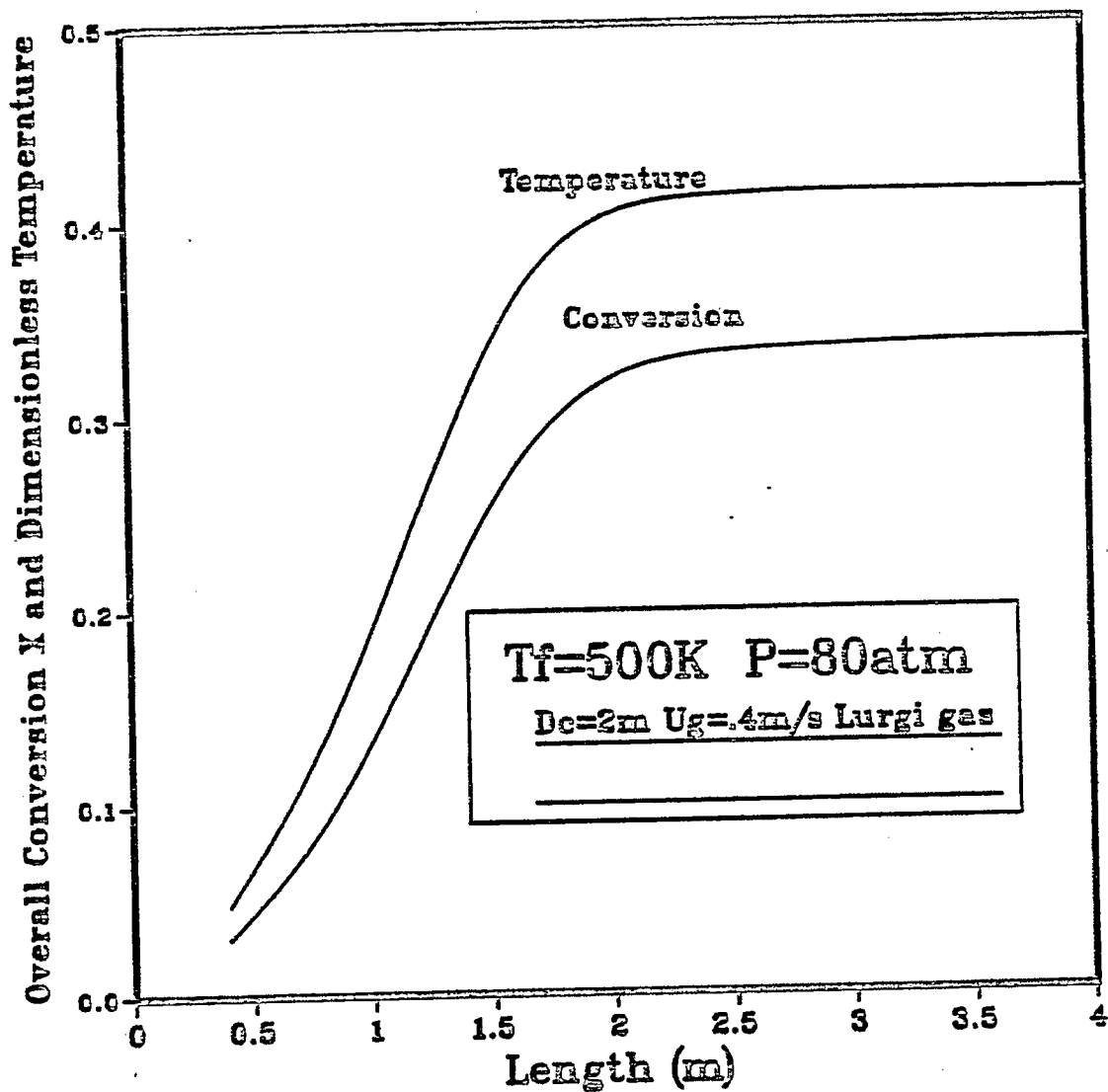


Figure I-C-6: Conversion and dimensionless temperature profiles for a fixed-bed methanol synthesis reactor

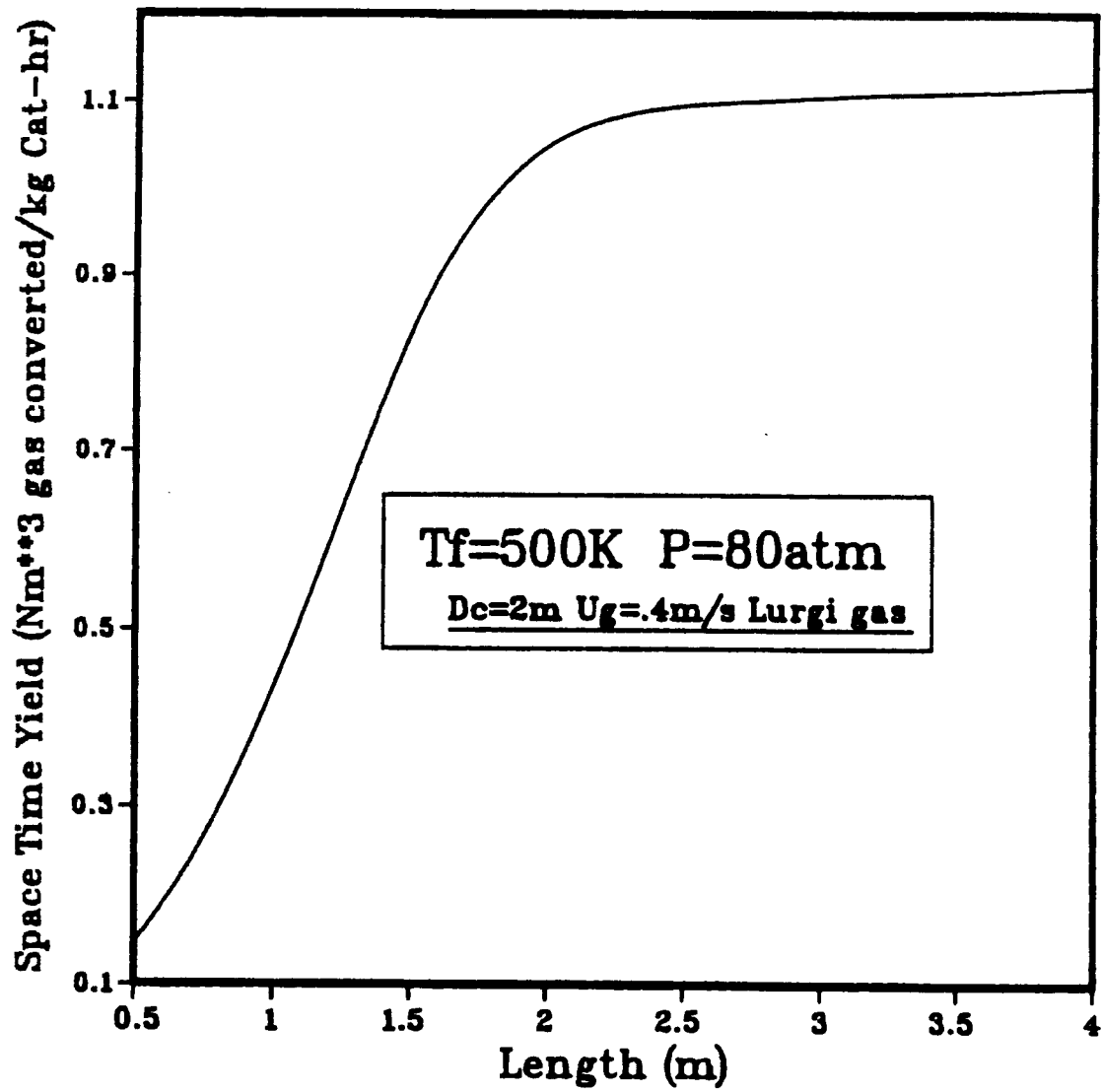


Figure I-C-7: Space time yield in fixed bed methanol synthesis reactor

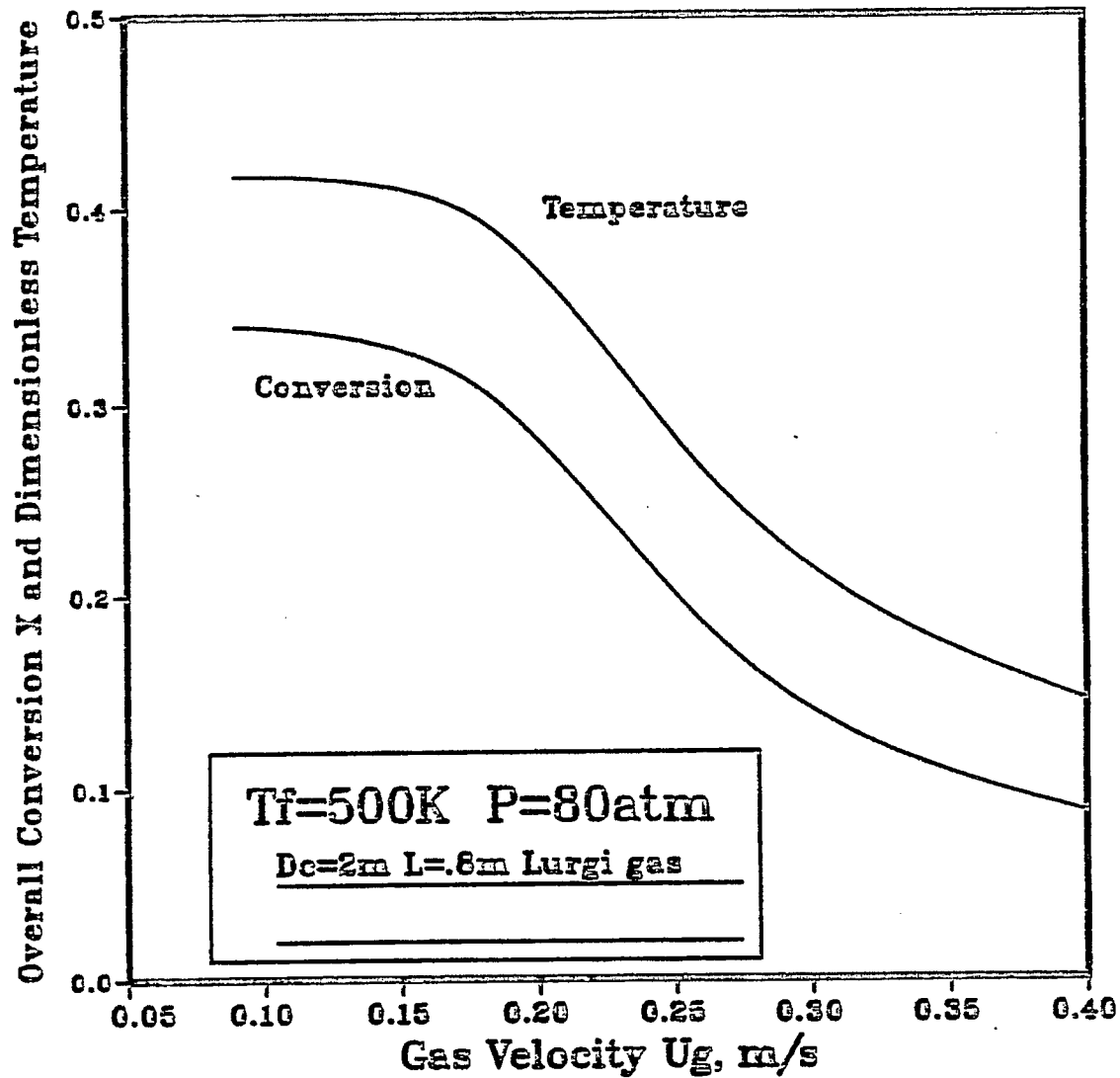


Figure I-C-8: Effect of gas velocity on temperature and conversion

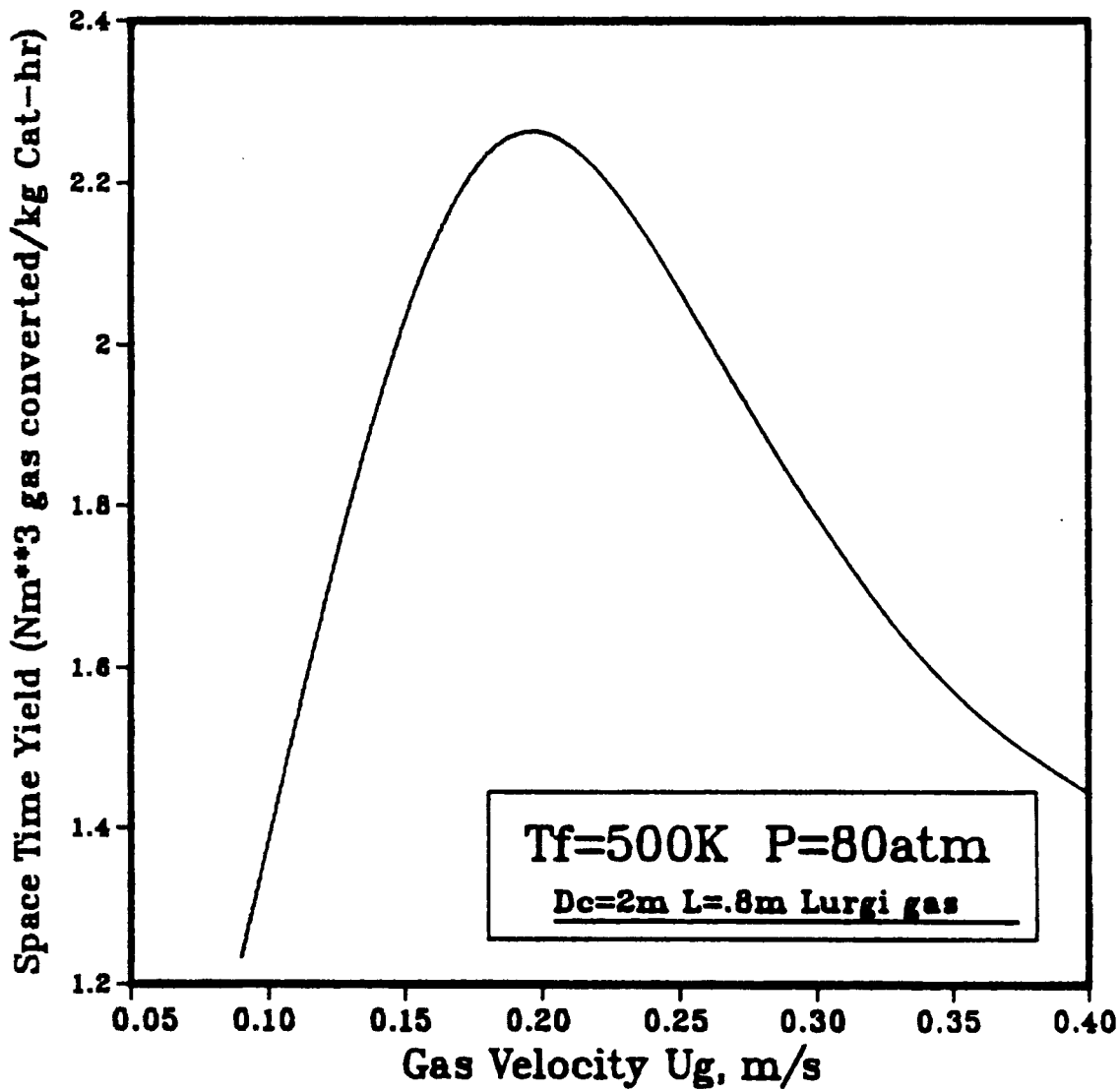


Figure I-C-9: Effect of gas velocity on STY

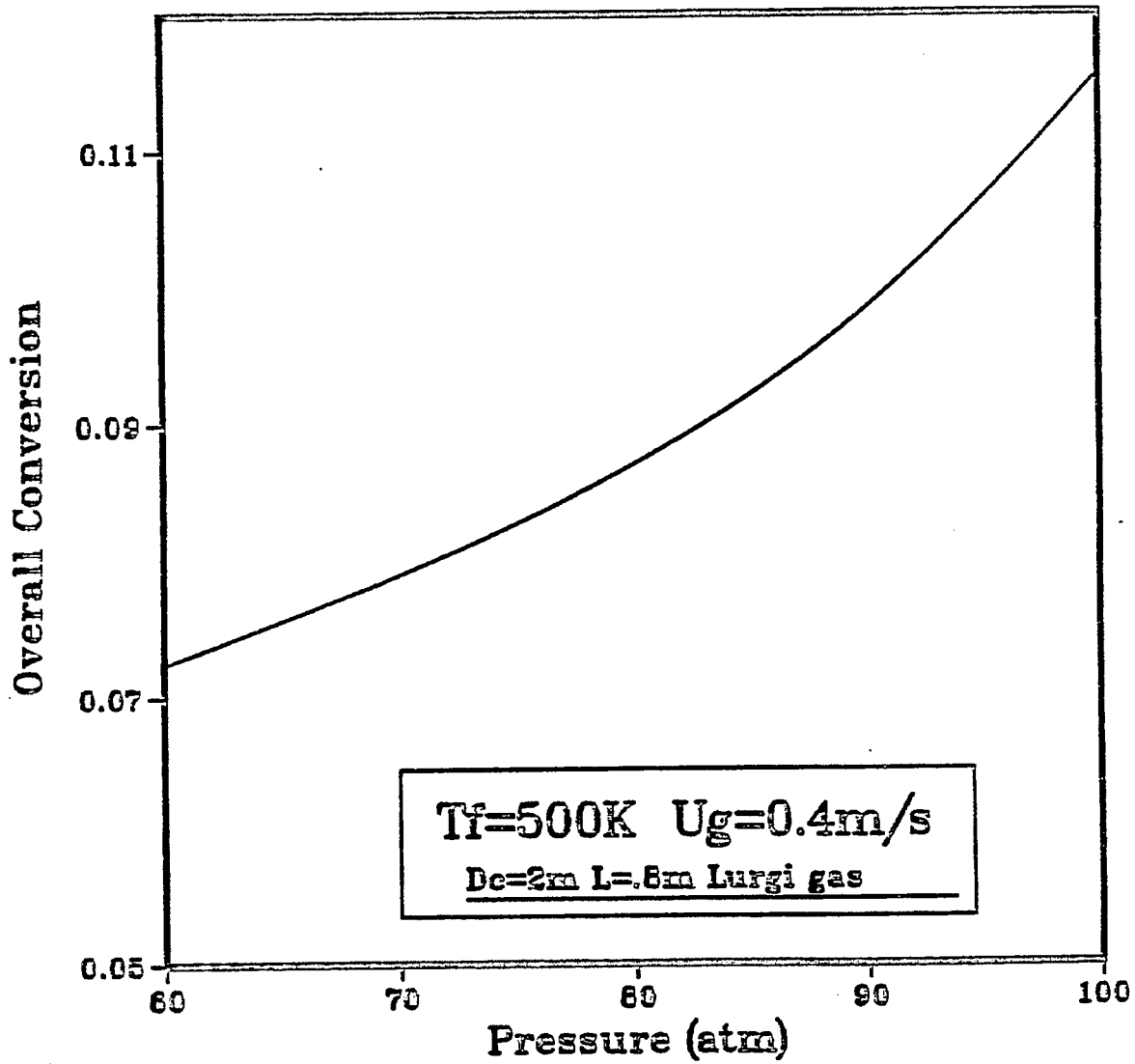


Figure I-C-10: Effect of pressure on conversion

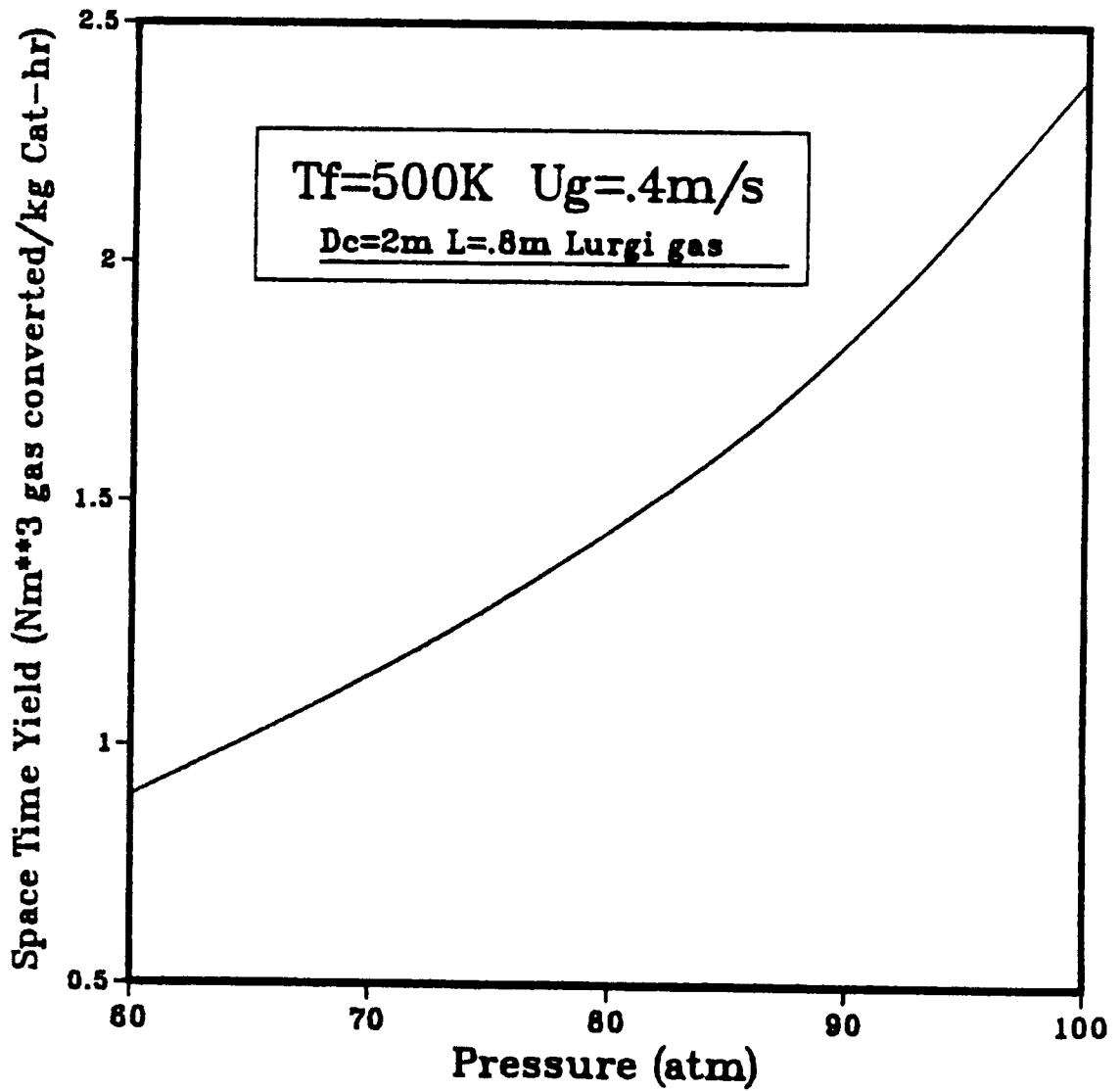


Figure I-C-11: Effect of pressure on STY

d. Effect of Inlet Temperature

Increase in inlet temperature leads to a gradual increase in conversion and STY. Figs. I-C-12 and I-C-13 summarize the results at 80 atm. This increase is, of course, due to the increase of the reaction rates and should be less pronounced after a certain value of temperature where equilibrium becomes important.

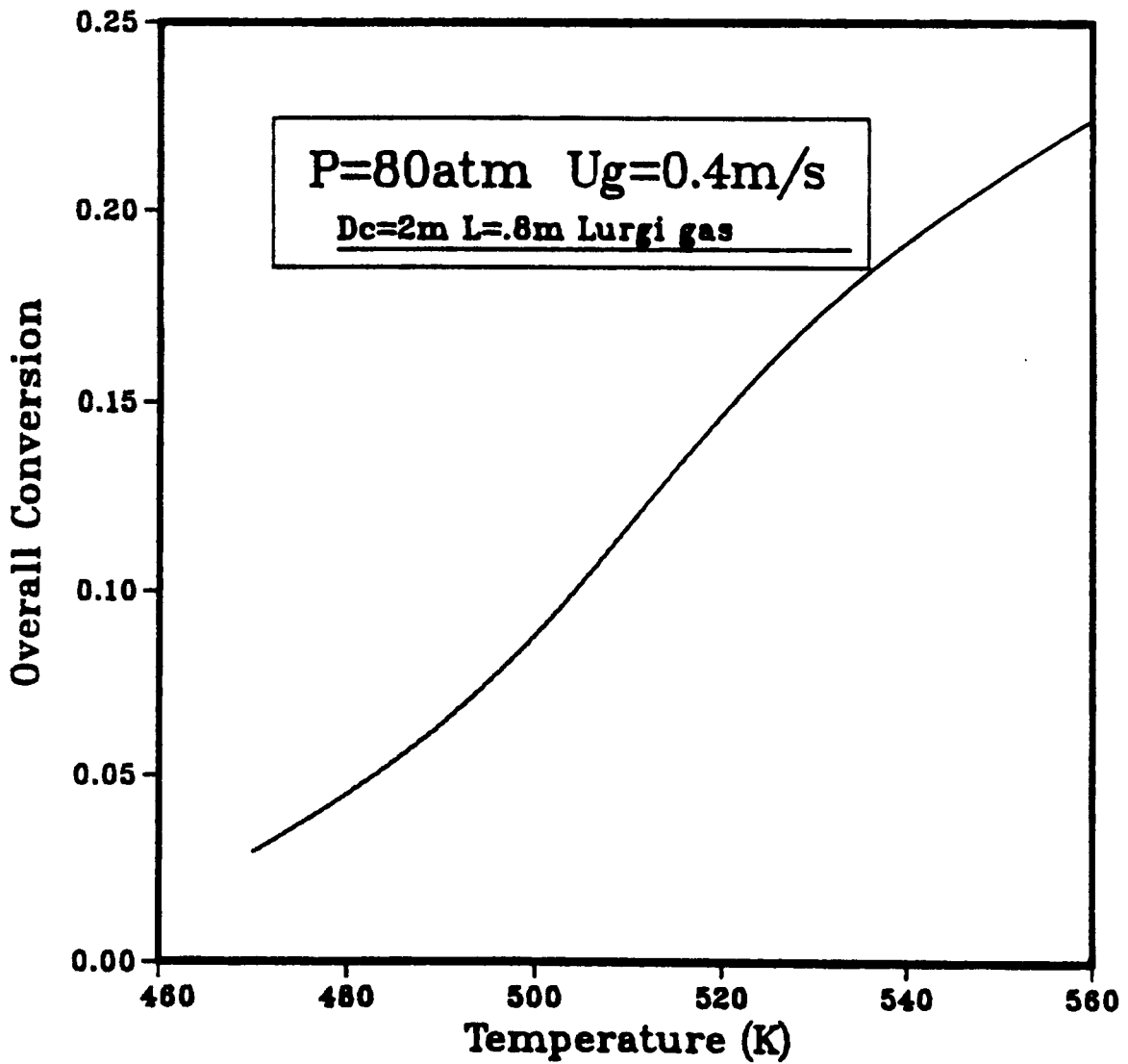


Figure I-C-12: Effect of feed temperature on conversion

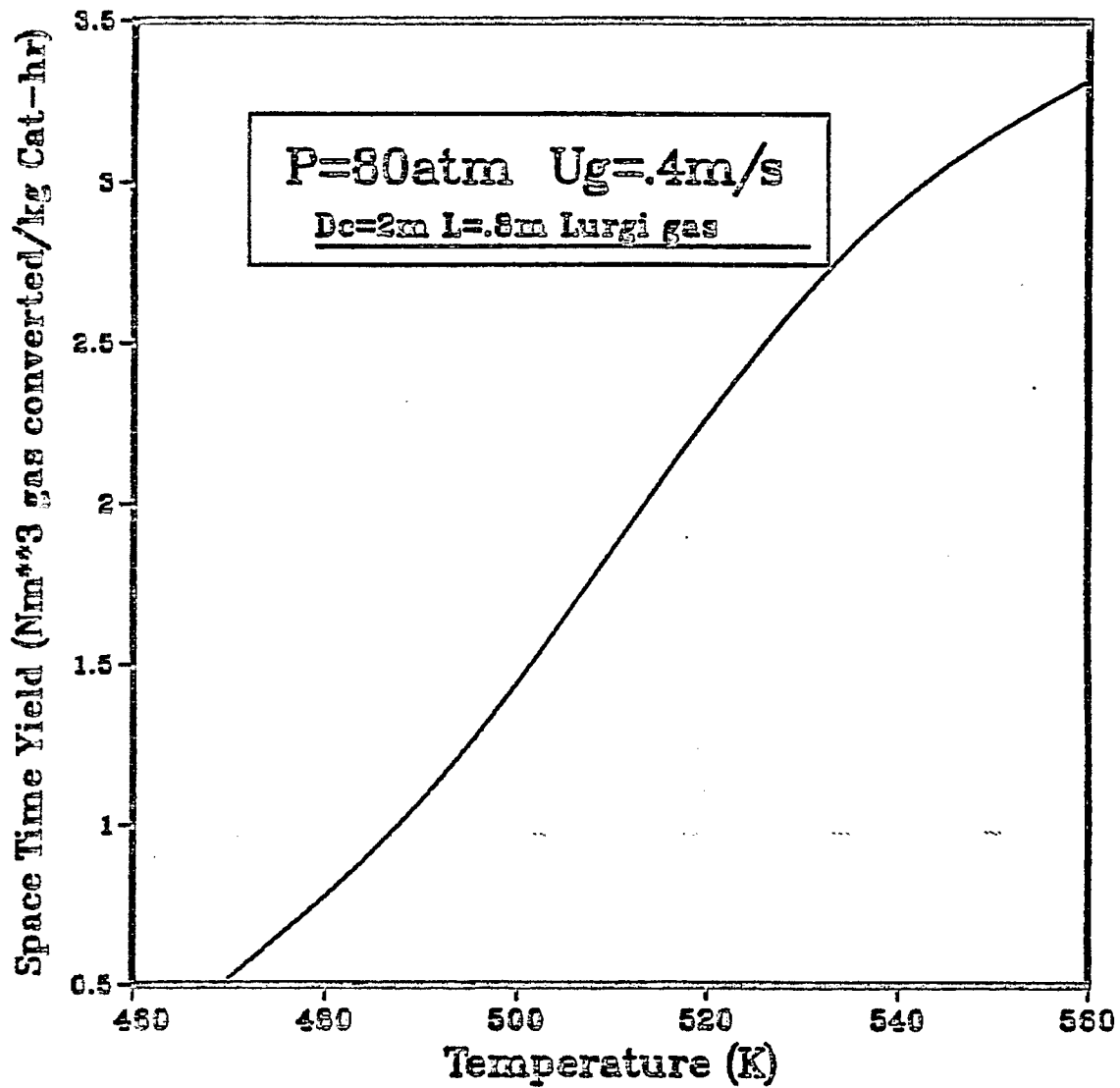


Figure I-C-13: Effect of feed temperature on STY

Slurry-Bed Reactor Design for Methanol Synthesis

The synthesis of methanol from hydrogen and carbon monoxide has been a focal point in synfuel research. Until recently, most of the investigations involved only two phases; the reactants and products forming the vapor phase and the catalyst representing the solid phase. With the development of more efficient catalysts, it has been possible to increase the rate of the synthesis reaction several fold. While this appears to be a welcome development it is not entirely without misgivings. The higher rate of reaction results in the faster evolution of exothermic heat leading to fears of potential thermal deactivation of the catalyst and thermal instability of reactor operation.

In recent years, it has been suggested that the reaction could be carried out in the liquid phase which would act as a temperature moderator in the reactor. The choice of a suitable liquid is dictated by the stability of the liquid at reaction temperature and pressure, a low vapor pressure at reaction conditions and the capacity to dissolve and permit the diffusion of gaseous reactants to the active sites. Furthermore, reactor economics necessitates the use of easily available and inexpensive liquids which can be pumped around the system at the least expense of energy. The liquids that appear promising are Witco-40 (a white mineral oil) and Freezene 100.

Because of simplicity of operation, low operating costs and ease with which liquid residence time can be varied, bubble-column slurry reactors have provided a range of applications in gas-liquid-solid reaction systems (Shah et al., 1982). This type of reactor holds the promise of improving the economics of methanol synthesis systems due to its ability to operate at very high conversions, which are close to equilibrium levels, while maintaining an essentially isothermal reactor.

Figure I-C-14 illustrates the functioning of the bubble-column slurry reactor within the synthesis section of a liquid phase methanol (LPMeOH) plant. Synthesis gas containing CO, CO₂ and H₂ is passed upward into the reactor concurrent with the slurry which absorbs the heat liberated during reaction. The slurry is separated from the vapor and recirculated to the bottom of the reactor via a heat exchanger, where cooling occurs by steam generation. The reactor effluent gases are cooled to condense the products and any inert hydrocarbon liquid which may be vaporized. Methanol and the inert hydrocarbon liquid are immiscible and are separated by a decanter. The methanol stream produced is suitable for fuel use directly or can be sent to a distillation unit (not shown) to produce chemical grade product. Unconverted gases are recycled back to the reactor. A small purge stream is taken off to limit the buildup of inerts which may be present in the synthesis gas feed (Sherwin and Frank, 1976).

The primary advantages of this system over current technology are:

i) Due to the excellent reaction temperature control, high per pass conversions of gas can be economically realized such that the methanol concentration in the reactor exit gas attains the 15-20 vol. % range as compared to a more normal figure of 2-6 vol. %. This in turn greatly reduces the recycle gas flow and compression requirement.

ii) The heat of reaction is largely recovered as high pressure steam in a simple manner.

iii) Reactor design is simplified in that liquids and gases are readily distributed across the reactor cross-sectional area without the necessity for redistribution and quench along the reactor length.

iv) Small size catalyst can be used, thereby achieving higher rates of reaction with larger catalyst particles.

I-212

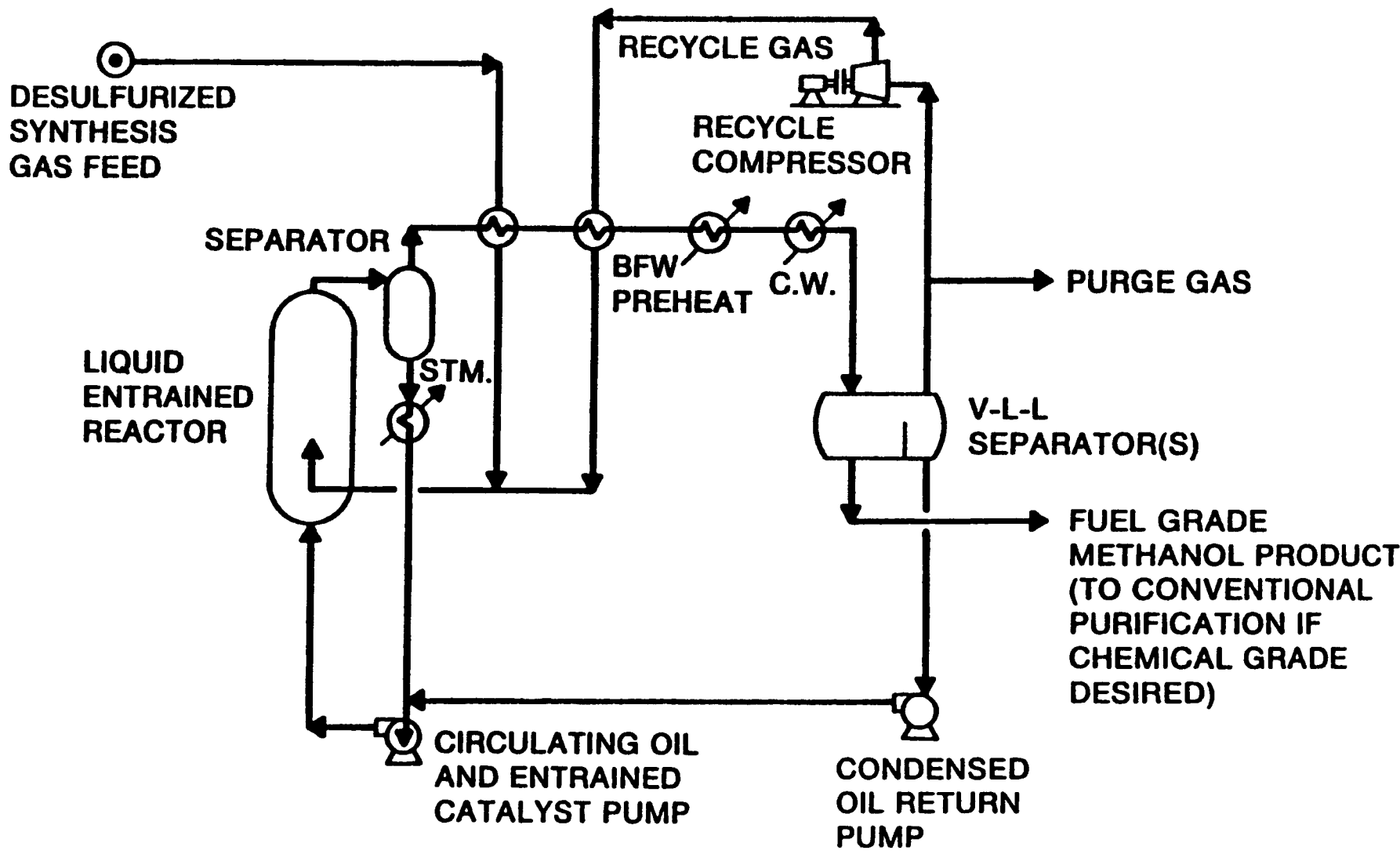


Figure I-C-14: Liquid phase methanol synthesis process (Sherwin and Frank, 1976)

v) Catalyst can be added and withdrawn from the system without the necessity of shutdown.

vi) The near isothermal temperature of the system permits optimum conditions favoring the desired reaction kinetics.

vii) Catalyst activity can be maintained at a constant "equilibrium" activity level so that it is not necessary to overdesign the reactor size for the "end of life" catalyst activity level.

Chem Systems Inc. have been developing the LPMeOH technology under the sponsorship of Electric Power Research Institute (EPRI) since 1975 (Sherwin and Blum, 1979). In 1981, Air Products and Chemicals, Inc. started a 42-month research and development program to prove the technical feasibility of LPMeOH (Brown and Greene, 1984). In these two projects bubble column slurry reactors are used and several aspects of the new technology have been investigated. With all the information available, it is essential to develop a reactor simulator to predict the performance of such a reactor configuration and this part of the project aims at this point: A bubble-column slurry reactor is designed for the LPMeOH synthesis.

In general, a slurry reactor design procedure requires:

- A correlation for the intrinsic reaction kinetics.
- Models for gas, liquid and solid distribution and mixing.
- Correlations for predicting gas/liquid and liquid/solid mass transfer. Combination of these correlations and models into a single system constitutes a reactor model.

In designing a slurry reactor, the goal is to optimize the height and diameter of a reactor vessel for a specified capacity. First, the design gas superficial velocity (U_G) is specified. The choice of U_G is influenced by several factors; too high a value could result in excessive gas holdup,

whereas too low a value can result in uneconomically "hockey-puck-shaped" reactors. Given an allowable gas velocity and design synthesis gas feed flow, the necessary reactor cross-sectional area and diameter can be calculated.

With the diameter established, the reactor height (and hence the volume) depends on three basic factors; space velocity, slurry loading, and gas holdup. The choice of space velocity (here expressed as Nm^3 per kg catalyst per hour) relates directly to reactor conversion through the kinetics and mass transfer correlations and this fixes the weight of the slurry loading, which is expressed in kg of catalyst per m^3 of oil. A higher design slurry loading will always result in a lower reactor volume, other things being equal. However, too high a loading will make a highly viscous slurry with increased risk of plugging lines, valves and heat exchanger tubes.

Given the slurry volume and the specified gas velocity and predicted gas holdup, the required reactor volume can be calculated.

In the present work, a computer program has been developed for the design of a bubble-column slurry reactor for the methanol synthesis. The program is established in a general manner so that any kind of rate expression depending on the catalyst can be used. The following sections are devoted to the development of model equations, their solution techniques and the discussion of the results obtained from the simulator. The parameters involved and their estimations are outlined in the end of this part of the report.

a. Model Assumptions

The model of methanol synthesis in the slurry phase is based on the following phenomena and assumptions:

- 1) The total pressure within the reactor is constant, i.e., the influence of hydrostatic head on gas expansion is neglected. Due to relatively high pressures used, this assumption should be reasonable.

ii) There is no heat transfer to the surrounding, e.e., the reactor operates under adiabatic conditions.

iii) The variation of gas flow rate across the column is neglected. It was thought that, the flow rate of gas decreases as the conversion increases, while it increases as the temperature increases and these effects should compensate each other.

iv) For the flow pattern in gas phase, a plug flow model is used. This corresponds to a general case in bubble column slurry reactors where the gas phase Bodenstein number is usually very high.

v) The effectiveness factors for the pore diffusion inside the catalyst particles are taken as unity. Due to the very small particles ($d_p < 100 \mu\text{m}$) used the diffusional limitations should be negligible, hence, the approximation should be reasonable.

vi) Again, due to very small particle size, the liquid-solid mass transfer resistances are neglected. In addition, no temperature difference between the catalyst and the liquid is assumed.

Besides these simplifications, the following detailed points are considered in the model development.

vii) The slurry phase is modeled by an axial dispersion model, the most appropriate model for bubble column reactors (Deckwer et al., 1983).

viii) The catalyst is not uniformly distributed over the entire suspension volume which is considered by introducing the sedimentation dispersion model (Cova, 1966, Kato et al., 1972).

ix) The hydrodynamic properties, i.e., gas holdup, interfacial area, heat and mass transfer coefficients and dispersion coefficients are assumed to be spatially independent.

x) Owing to the low heat capacity of the gas phase compare to the slurry phase, a heat balance on the suspension (liquid plus solid) will only be considered.

xi) The physico-chemical properties (i.e., density, viscosity, diffusivity, and solubility) are considered to be a function of temperature.

xii) Both reactions, methanol formation and hydrogenation of CO₂ are considered.

b. Model Equations

Based on the above assumptions the following mass and energy balances can be written:

1. Mass Balances:

For ith component where

i = 1 for CO, 2 for CO₂, 3 for H₂, 4 for CH₃OH and 5 for H₂O

(a) Gas phase:

$$\frac{d}{dx} (U_G C_{ig}) + (k_L a)_i (C_{ig}^* - C_{il}) = 0 \quad (83)$$

using the following definitions and groups:

$$C_{ig}^* = P_i/H_i = P y_i/H_i \quad (83a)$$

$$C_{ig} = C_G y_i; C_G = P/RT \quad (83b)$$

$$z = x/L \quad (83c)$$

$$(St_G)_i = \frac{(k_L a)_{iL} RT_f}{U_G H_i} \quad (83d)$$

$$\theta = (T - T_f)/T_f \quad (83e)$$

$$x_i = \frac{H_i C_{iL}}{P} \quad (83f)$$

we get a dimensionless equation for gas phase mass balance:

$$\frac{dy_i}{dz} + (1 + \theta)(St_G)_i (y_i - x_i) = 0 \quad (84)$$

(b) Liquid Phase:

In the cocurrent operation, a differential mass balance yields:

$$\frac{d}{dx} (\epsilon_{LL} D_L \frac{d C_{iL}}{dx}) - \frac{d}{dx} (U_L C_{iL}) + (k_L a)_{iL} (C_{ig}^* - C_{iL}) + \sum_k v_{ik} \epsilon_{L cat}^r r_k = 0 \quad (85)$$

Here v_{ik} is the stoichiometric coefficient for component i , for reaction k . For products v_{ik} is positive and for reactants it should be negative.

Using the following definitions and groups:

$$(St_L)_i = \frac{(k_L a)_{iL} L}{U_G} \quad (85a)$$

$$Bo_L = \frac{U_G L}{\epsilon_{LL} D_L} \quad (85b)$$

$$q = U_L / U_G \quad (85c)$$

$$\psi = C_{cat} / C_{cat,f} \quad (85d)$$

$$\phi_{ik} = \frac{r_k H_i}{k_k P} v_{ik} \quad (85e)$$

$$Da_k = \frac{\epsilon_L C_{cat,f} L}{U_G} k_k \quad (85f)$$

we get the following dimensionless equation for liquid phase mass balance

$$\frac{1}{Bo_L} \frac{d^2 x_i}{dz^2} - q \frac{dx_i}{dz} + (St_L)_i (y_i - x_i) + \sum_k \psi Da_k \phi_{ik} = 0 \quad (86)$$

2. Solid catalyst balance:

Using sedimentation dispersion model we can write:

$$D_s \frac{d^2 C_{cat}}{dx^2} + (U_{ss} - \frac{U_L}{1 - \epsilon_G}) \frac{dC_{cat}}{dx} = 0 \quad (87)$$

integration with suitable boundary conditions results in

$$\psi = \frac{C_{cat}}{C_{cat,f}} = \frac{Bo_s \exp[(Bo_s - Bo_L^*)(1-z)] - Bo_L^*}{Bo_s - Bo_L^*} \quad (88)$$

with $Bo_s = \frac{U_{ss} L}{D_s} \quad (88a)$

and $Bo_L^* = \frac{U_L L}{D_s (1 - \epsilon_G)} \quad (88b)$

3. Energy Balance

Considering the slurry phase as pseudohomogeneous, we can write the following balance for adiabatic case:

$$\frac{d}{dx} (\epsilon_L \lambda \frac{dT}{dx}) - \frac{d}{dx} (U_g \bar{\rho} \bar{C}_p T) + \sum_k \epsilon_L C_{cat} r_k (-\Delta H_R)_k = 0 \quad (89)$$

using:

$$\theta = (T - T_f)/T_f \quad (89a)$$

$$Pe = \frac{U_g \bar{\rho} \bar{C}_p L}{\epsilon_{SL} \lambda} \quad (89b)$$

$$Be_{i,k} = \frac{(-\Delta H_R)_k P}{\bar{\rho} \bar{C}_{p,i} T_f v_{ik}} \quad (89c)$$

we get the following dimensionless equation

$$\frac{1}{Pe} \frac{d^2 \theta}{dz^2} - q \frac{d\theta}{dz} + \sum_k \psi Be_{ik} Da_k \phi_{ik} = 0 \quad (90)$$

The final form of the mass and energy balance equations are subject to the following boundary conditions:

$$\text{@ } z = 0 \quad y_i = y_{i,f} \quad (91)$$

$$x_i = x_{i,f} + \frac{1}{Bo_L} \frac{dx_i}{dz} \quad (92)$$

$$\theta = \frac{1}{Bo_L} \frac{d\theta}{dz} \quad (93)$$

$$\text{@ } z = 1 \quad \frac{dx_1}{dz} = \frac{d\theta}{dz} = 0 \quad (94)$$

c. Solution Technique

The system of eleven differential equations (five for gas and liquid phase mass balances plus one for energy balance) which presents the design model is nonlinear and subject to boundary conditions. For the solution of model equations numerically, the method of orthogonal collocation was used. A computer software, COLSYS (Ascher et al., 1981) which uses B-spline collocation functions was applied. As a rule, the collocation was done for four inner points.

The program developed calculates the profiles of the following quantities; gas and liquid phase concentrations, temperature, catalyst concentration and conversions. The conversions are defined as:

$$X_1 = \text{conversion for methanol formation reaction}$$

$$= \frac{N_{\text{CH}_3\text{OH}}^{\circ} - N_{\text{CH}_3\text{OH}}}{N_{\text{CO}}^{\circ}} - \frac{N_{\text{CO}_2}^{\circ} - N_{\text{CO}_2}}{N_{\text{CO}}^{\circ}} \quad (95)$$

and

$$X_2 = \text{conversion for hydrogenation of CO}_2$$

$$= \frac{N_{\text{CO}_2}^{\circ} - N_{\text{CO}}}{N_{\text{CO}}^{\circ}} \quad (96)$$

where N_1 represents the total (gas plus liquid) molar flow rate of the species. The overall conversion is defined as

$$X_{\text{overall}} = X_1 + X_2 = \frac{N_{\text{CH}_3\text{OH}} - N_{\text{CH}_3\text{OH}}^0}{N_{\text{CO}}^0} \quad (97)$$

In addition to the above mentioned quantities space-time-yield, STY in Nm³ synthesis gas converted per hour and kg catalyst in the reactor were computed.

d. Parameter Effect on Reactor Performance

The design model involves numerous quantities which may influence the performance of bubble column slurry reactor for methanol synthesis. In this part a parametric study was performed to test the simulator and to investigate the reactor behavior under a set of operating and design parameters.

The computations were done for a large scale reactor and the results are presented in graphical forms. The trends are discussed based on theoretical considerations.

The concentration profiles (mole fractions for gas phase and dimensionless concentrations for liquid phase) are shown in Fig. I-C-15 for a reactor of 1 m diameter and 8 m length. The liquid phase profiles were found to be relatively flat showing that dispersion is appreciable. The difference between gas and liquid phase concentration is small and it can be seen that the liquid phase is saturated after a dimensionless length of 0.2. As it will be seen later, the methanol synthesis in slurry reactor is kinetically controlled hence the liquid phase concentration corresponds to equilibrium (saturation) value. The concentrations decreases only because of the reaction.

The conversions for methanol formation and shift reaction are presented in Fig. I-C-16. Both of them increase with axial coordinate and neither of them reach equilibrium. Although the contribution of shift reaction is very small (0.025%), it is not negligible.

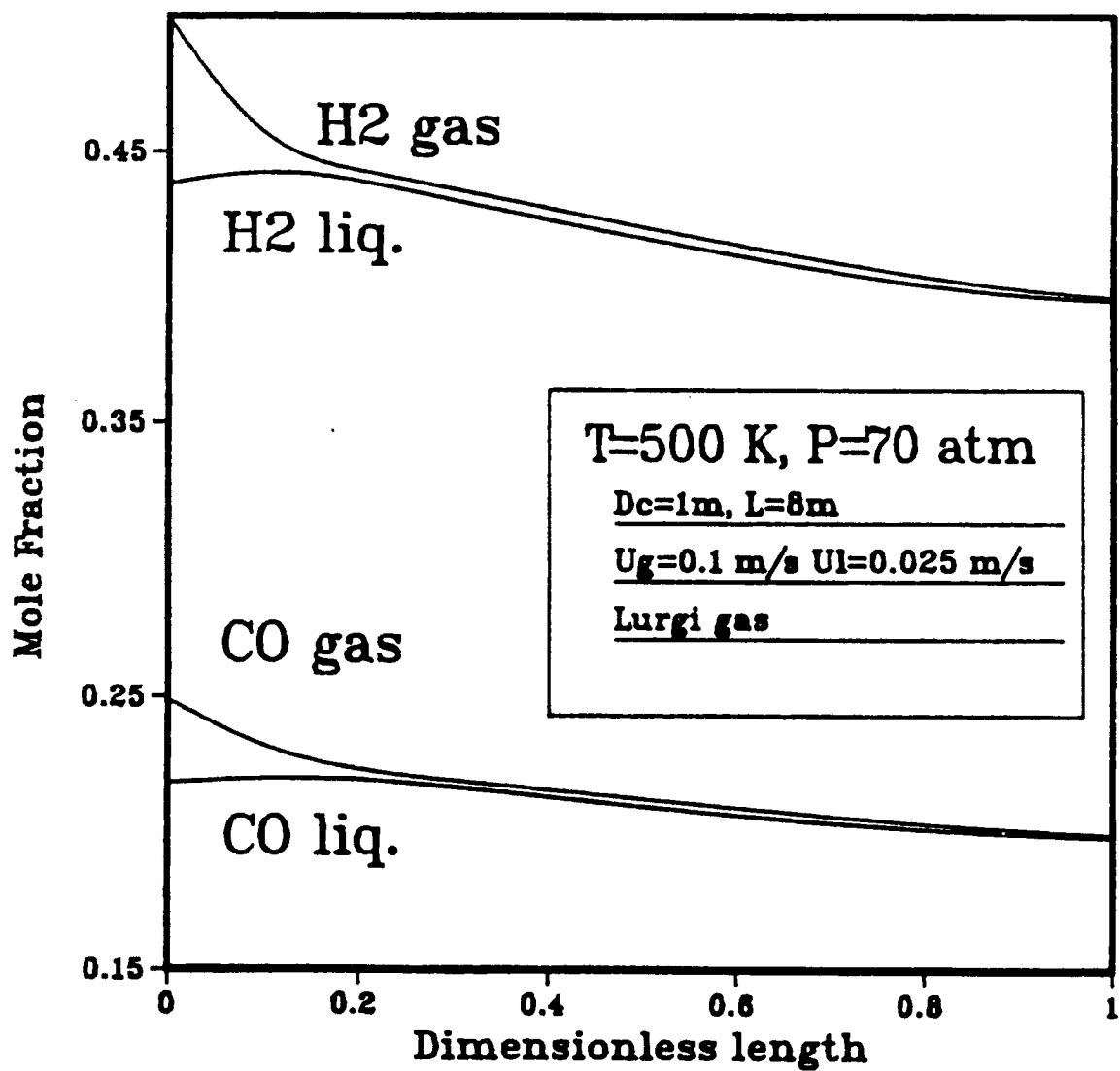


Figure I-C-15: Concentration profiles in a bubble column slurry reactor

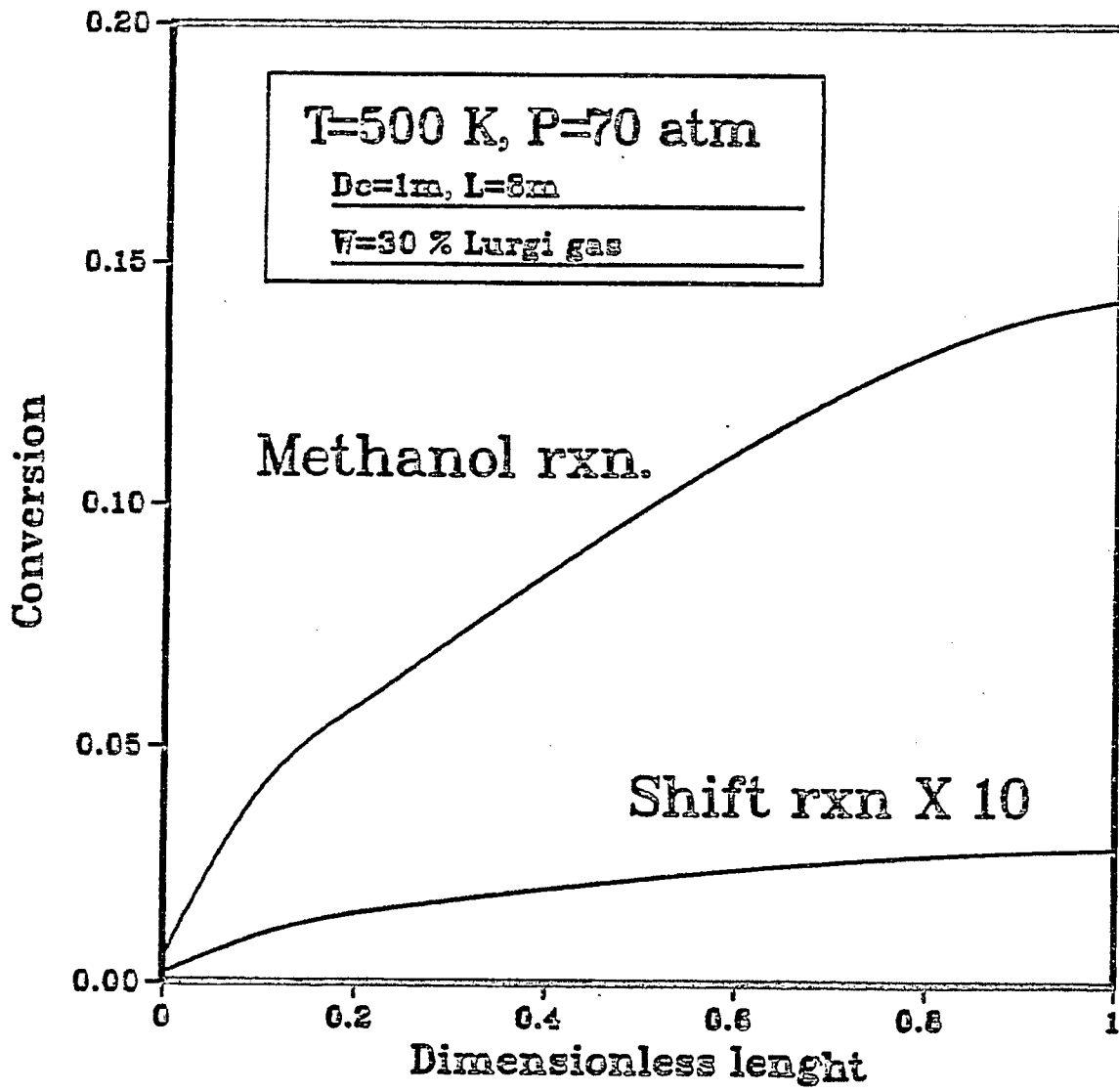


Figure I-C-16: Conversion profile in a bubble column slurry reactor

A very flat temperature profile was observed for temperature (Fig I-C-17) while a relatively high dispersion was obtained in catalyst concentration. In general they are very flat and the dispersion should be high enough. Catalyst concentration is always higher than the feed concentration but it reaches the feed concentration at the exit of the reactor. Therefore no accumulation is expected.

a. Effect of Column Diameter

The column diameter was varied between 1 and 4 m. The results are presented in Figs. I-C-18 and I-C-19 for conversion and Space Time Yield (STY) respectively. A slight decrease is found when increasing the diameter. As the dispersion coefficients are mainly affected by diameter, the decrease has to be attributed to enlarged dispersion in liquid phase. The overall effect is only moderate however its consideration should be very important in scale up of slurry reactors (Shah and Deckwer, 1985).

b. Effect of Column Height

Increase in the column height leads to a gradual increase in both conversion and STY. This is due to the fact that residence time of the gas and liquid in the reactor increases. The results are shown in Figs. I-C-20 and I-C-21.

c. Effect of Slurry Velocity

The slurry velocity was found to be a very important factor affecting the performance. As it can be seen from Figs. I-C-22 and I-C-23) both the conversion and STY increase drastically. Obviously, the reaction phase is liquid (slurry) phase and the increase in the flow rate decreases the residence time and the conversion. At low slurry flow rates, the temperature of the reactor increases to very high values since the rate of heat removal

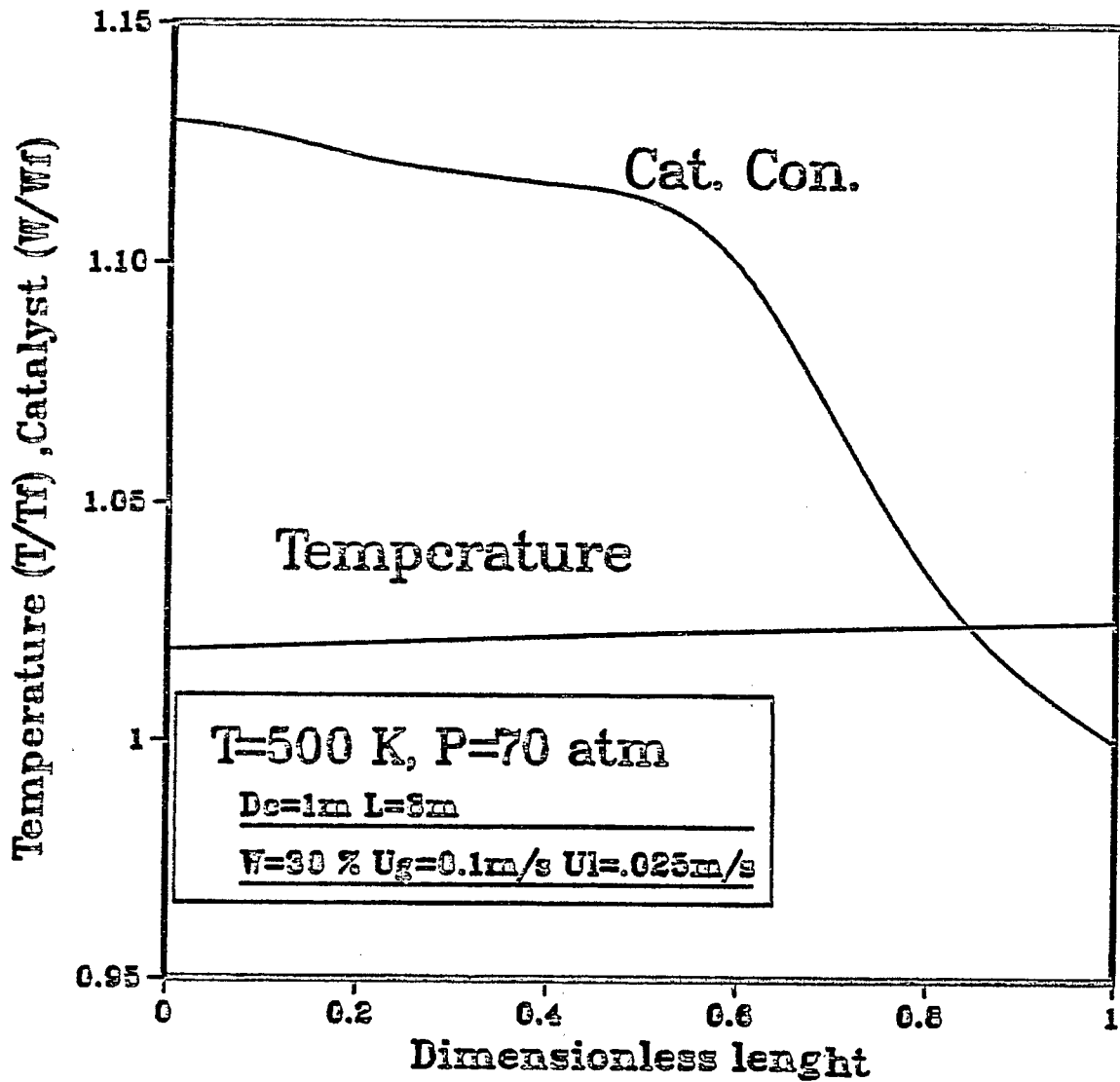


Figure I-C-17: Temperature and catalyst concentration profiles

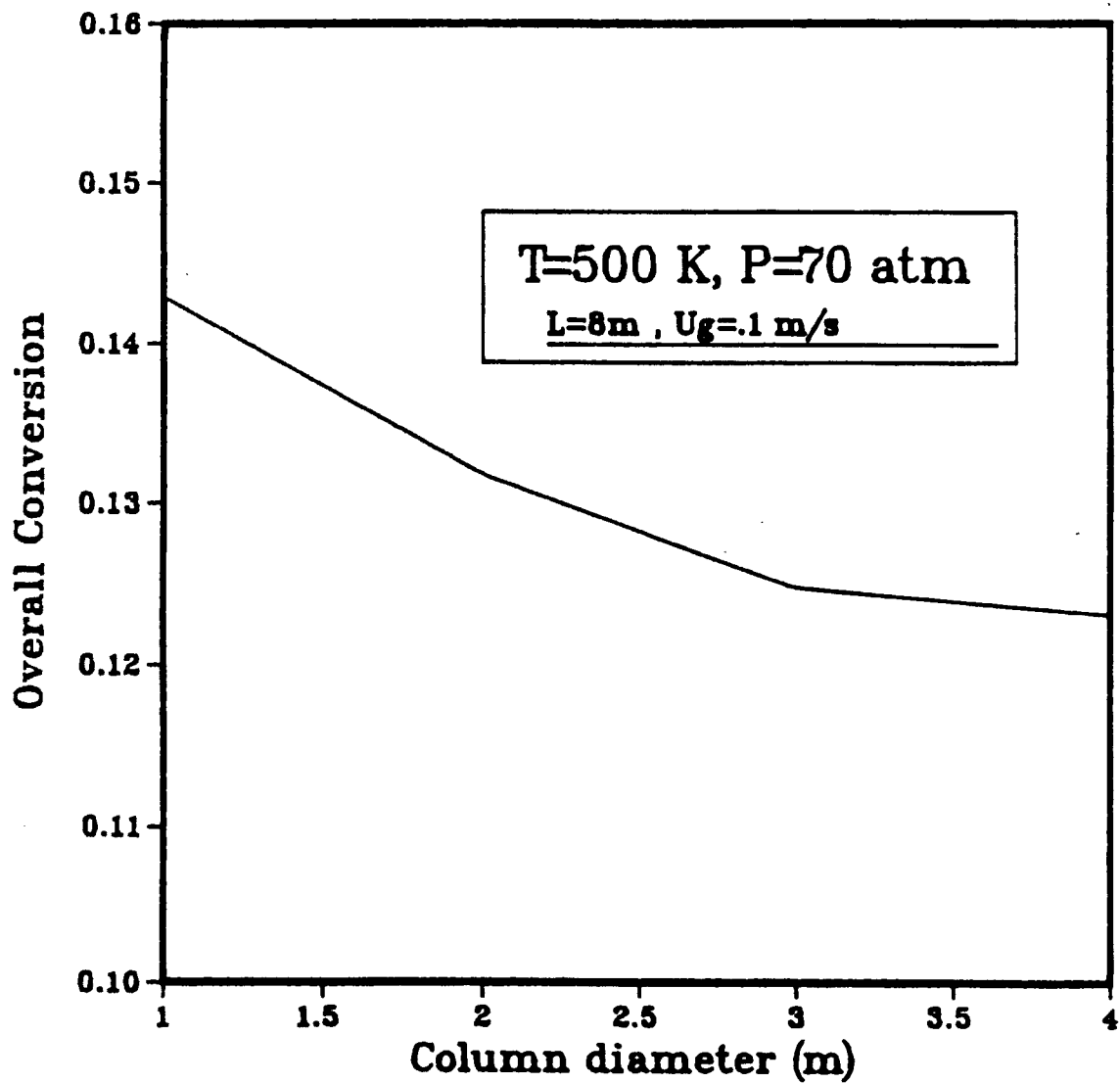


Figure I-C-18: Effect of column diameters on conversion

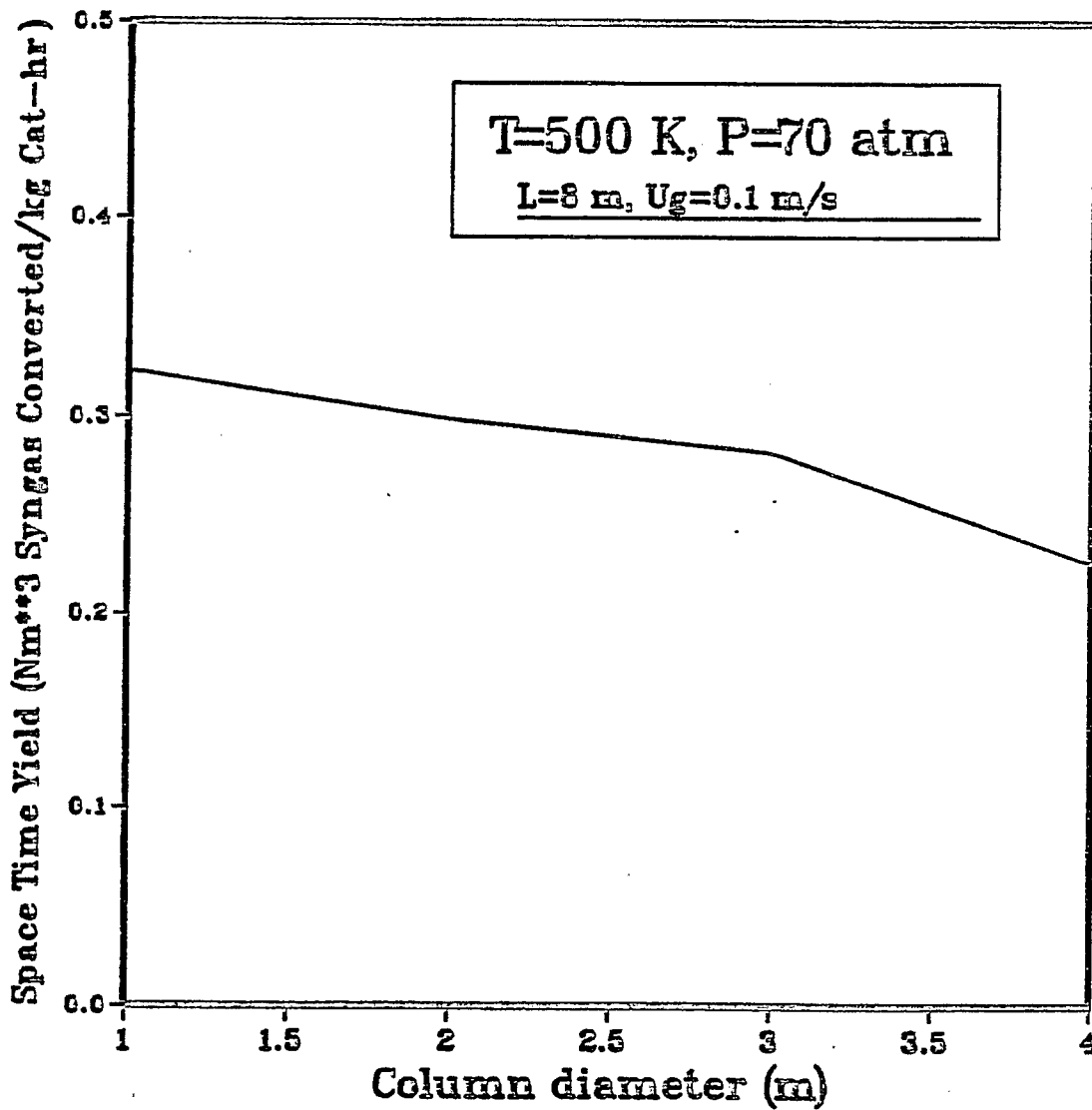


Figure I-C-19: Effect of column diameter on STY

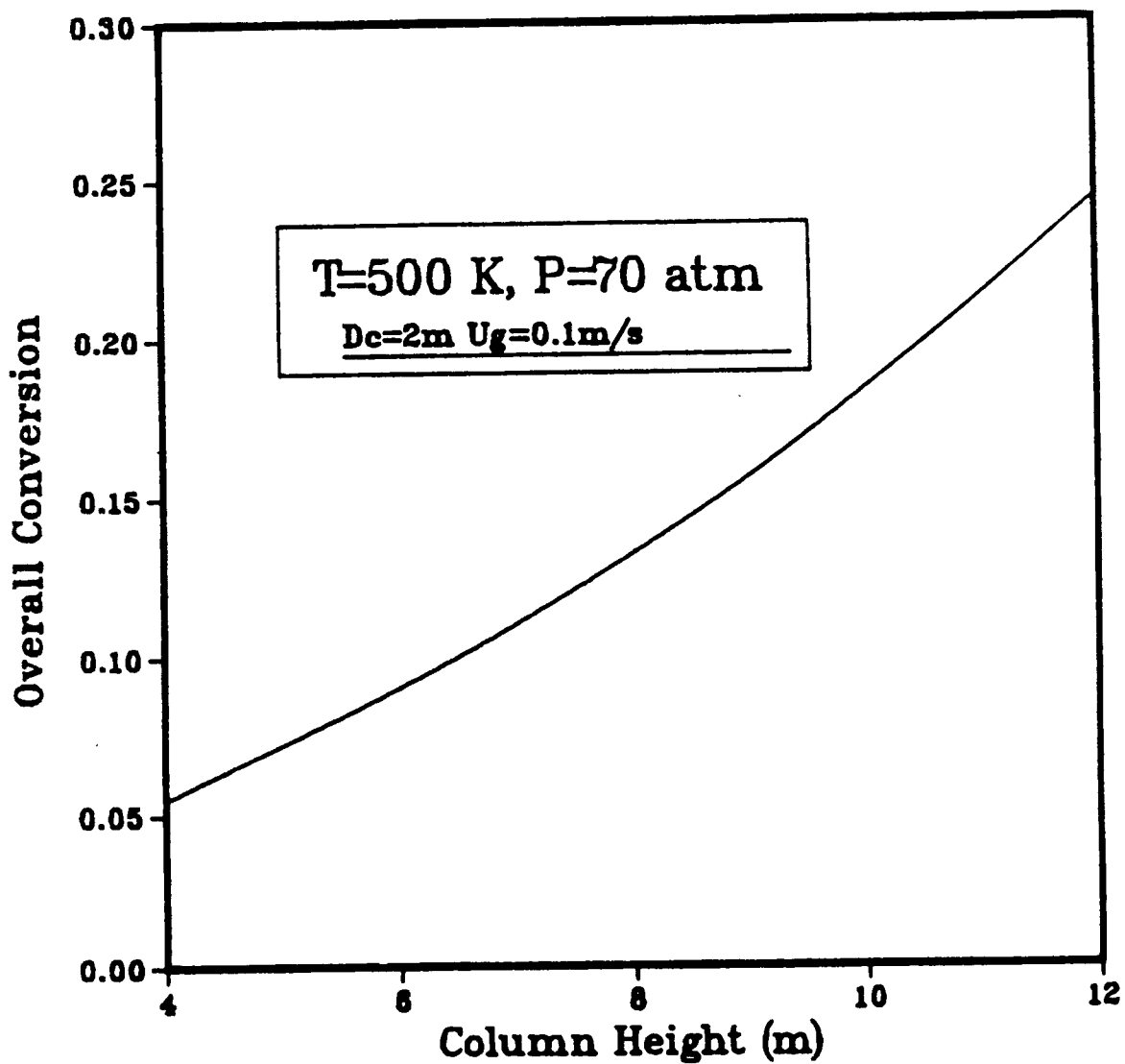


Figure I-C-20: Effect of column height on conversion

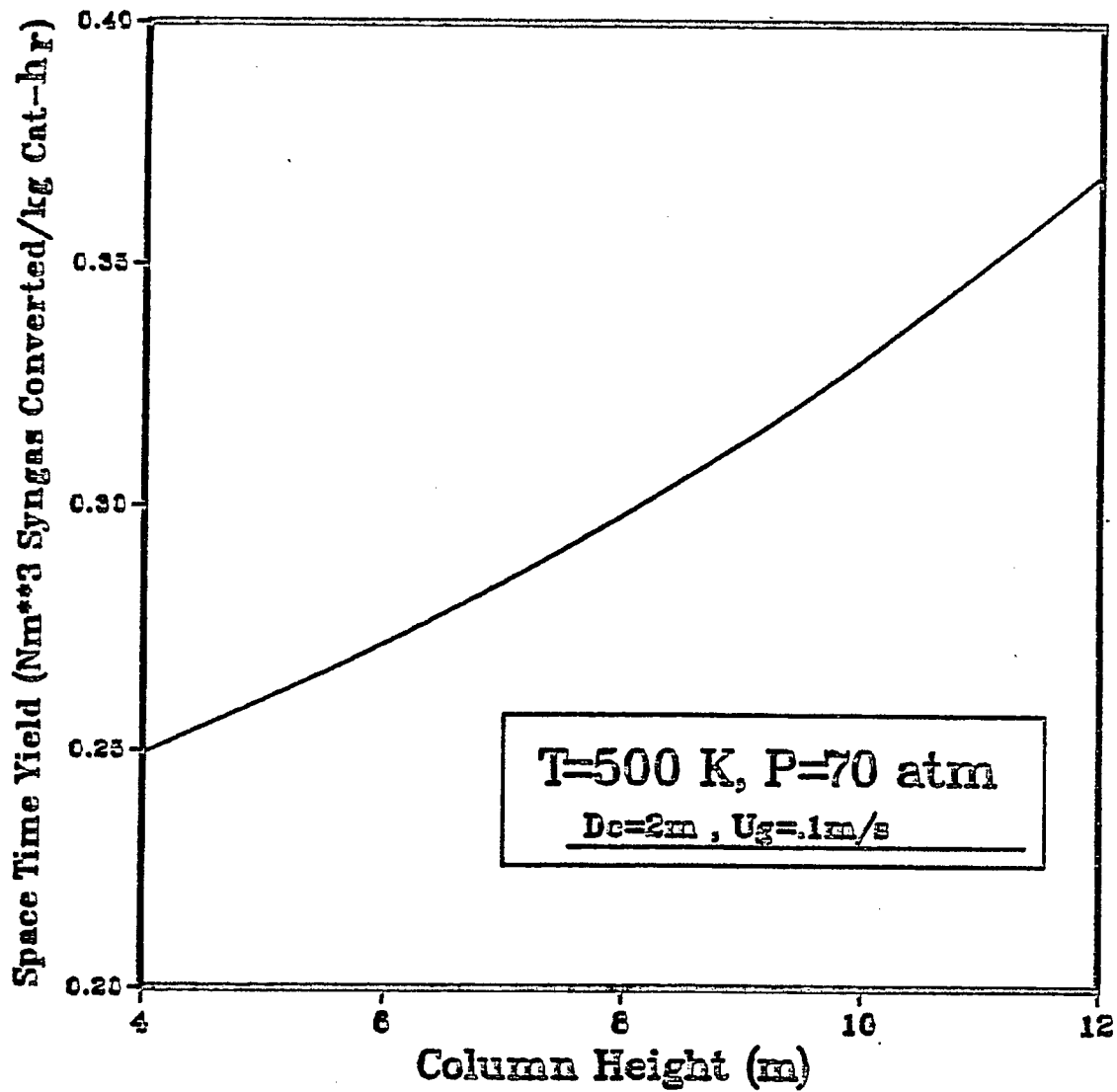


Figure I-C-21: Effect of column height on STY

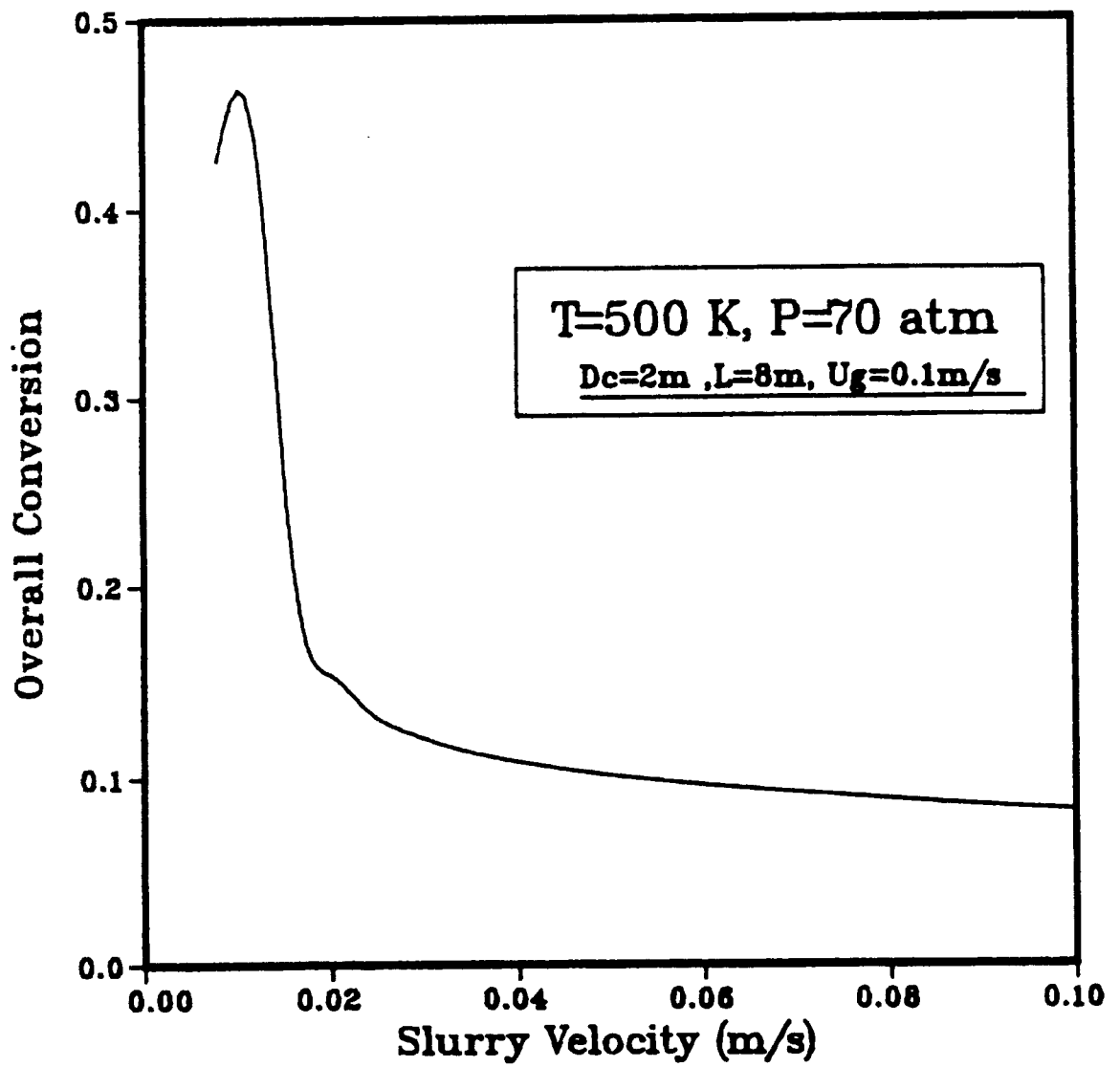


Figure I-C-22: Effect of slurry velocity on conversion

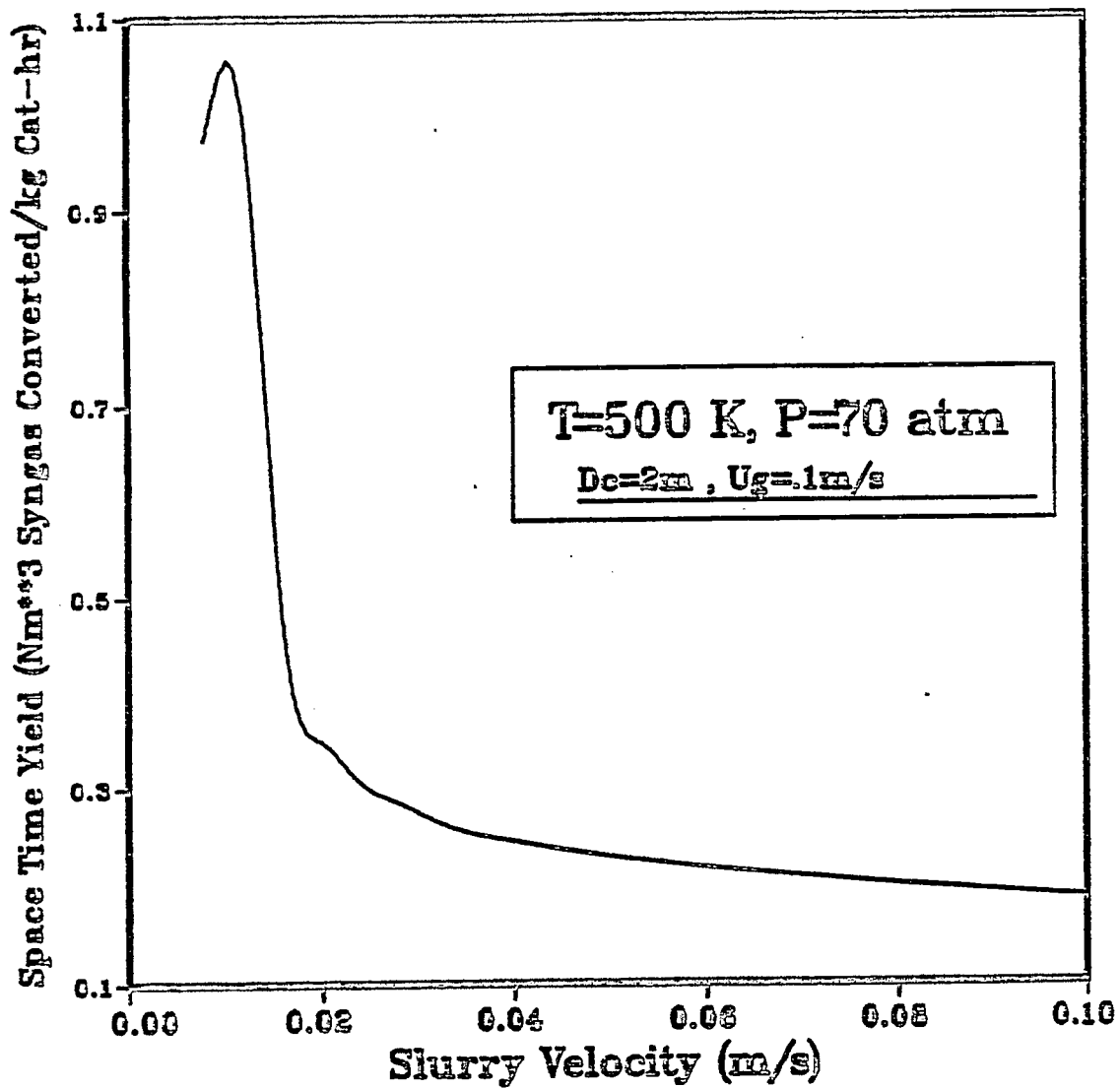


Figure I-C-23: Effect of slurry velocity on STY

decreases. Hence it is safer to operate the reactor at higher slurry velocities but the drop in conversion should also be taken into account.

d. Effect of Gas Velocity and Catalyst Loading

Increase in the gas velocity leads to a gradual drop in conversion but to a gradual increase in Space Time Yield (STY). The results are presented in Figs. I-C-24 and I-C-25 for different catalyst loadings. It is apparent that the reaction is kinetically controlled since conversion increases directly with catalyst concentration. At low gas velocities STY increases with decreasing catalyst loading showing that mass transfer resistances can be important and the effect of catalyst loading increases the slurry viscosity leading to a decrease in mass transfer coefficients.

e. Effect of Inlet Temperature

Both conversion and STY increases with inlet temperature. The S shaped figures shows that (Figs. I-C-26 and I-C-27) the reaction reaches at equilibrium after a certain temperature.

f. Effect of Pressure

The effect of pressure was studied for a pressure range of 50 to 100 atm. A gradual increase in conversion and STY was observed. The increases are not linear showing the effect of nonlinear rate expressions. Figs. I-C-28 and I-C-29 depict this behavior.

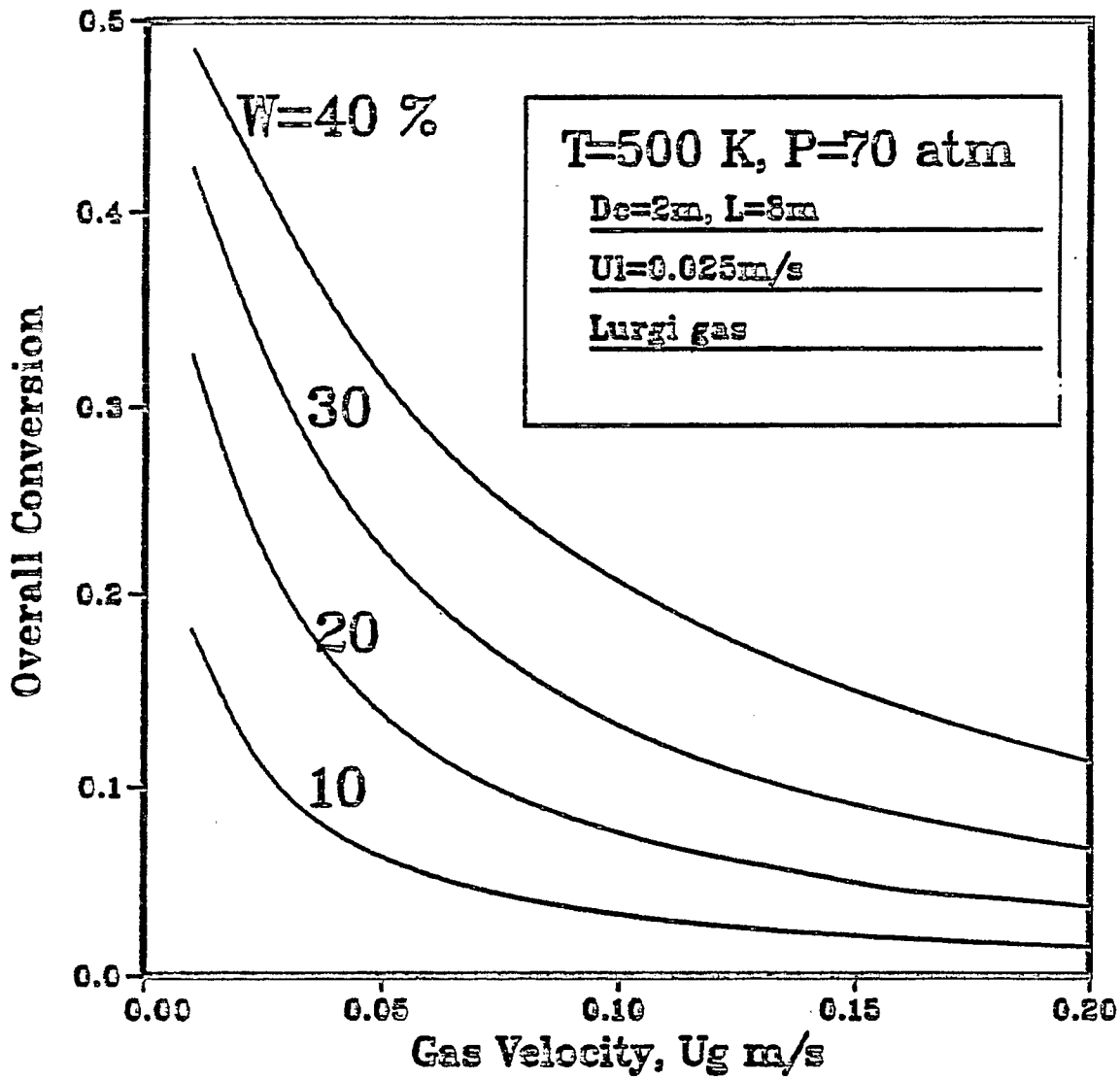


Figure I-C-24: Effect of gas velocity and catalyst loading on conversion

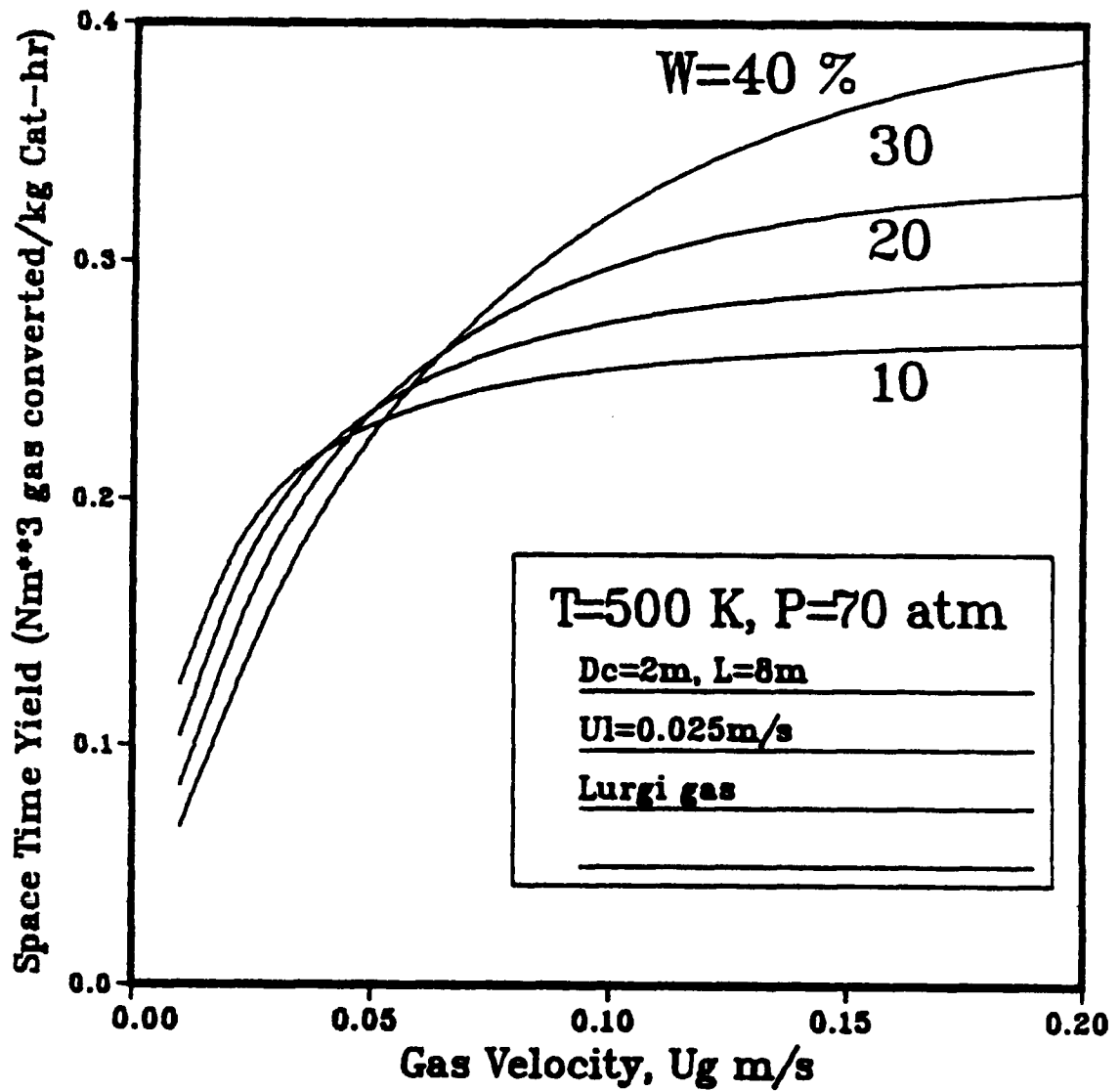


Figure I-C-25: Effect of gas velocity and catalyst loading on STY

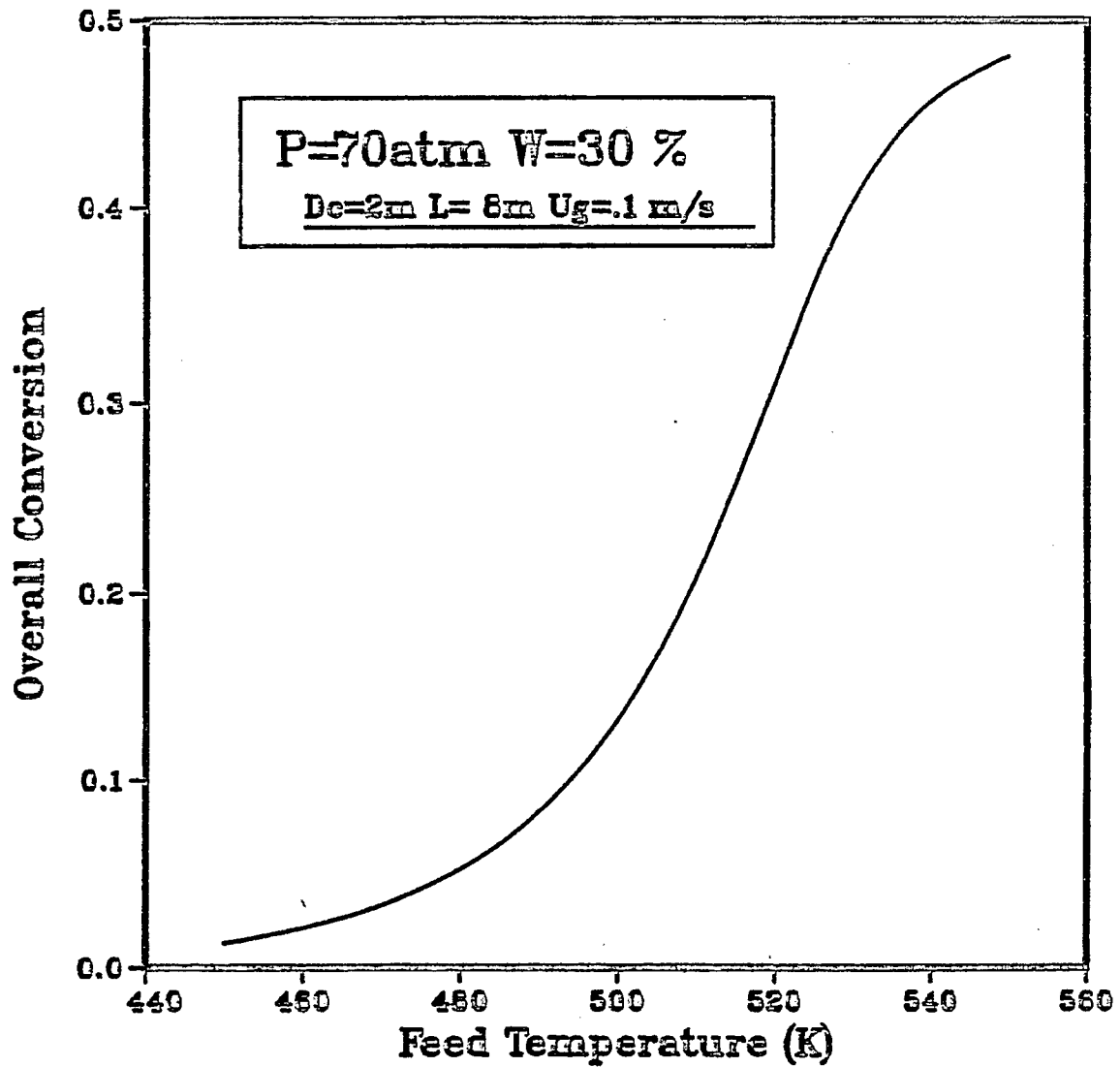


Figure I-C-26: Effect of temperature on conversion

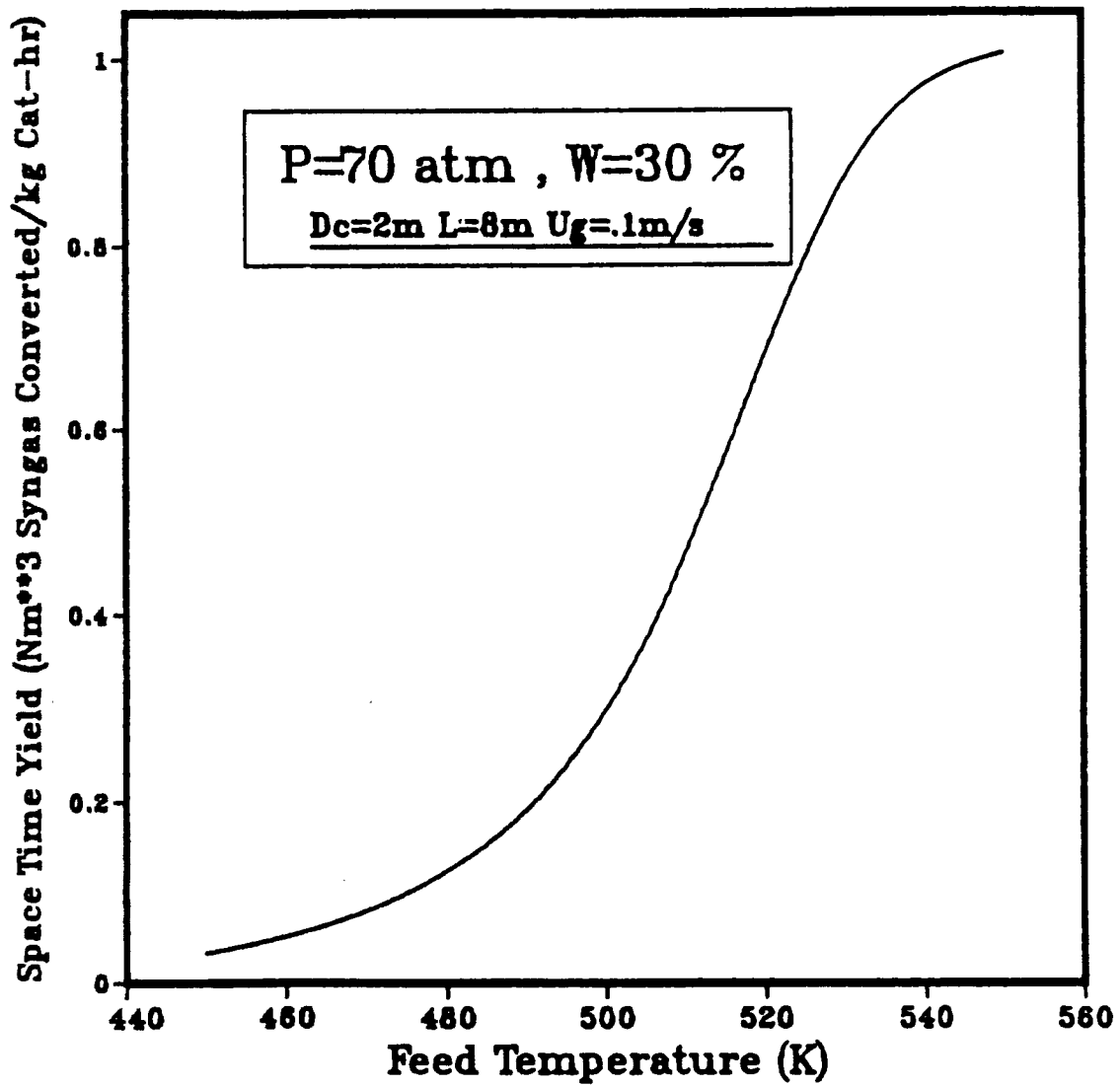


Figure I-C-27: Effect of temperature on STY

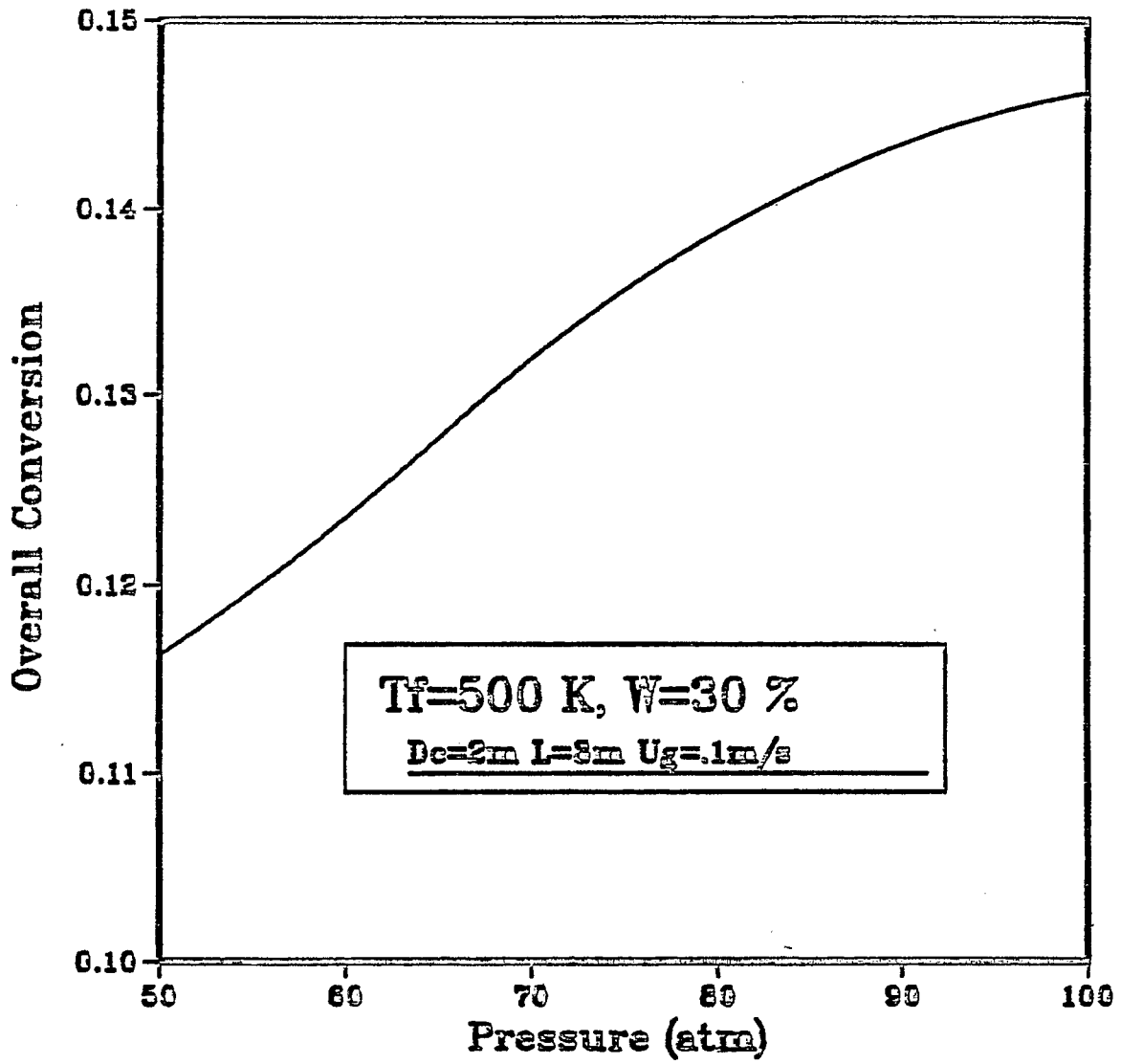


Figure I-C-28: Effect of pressure on conversion

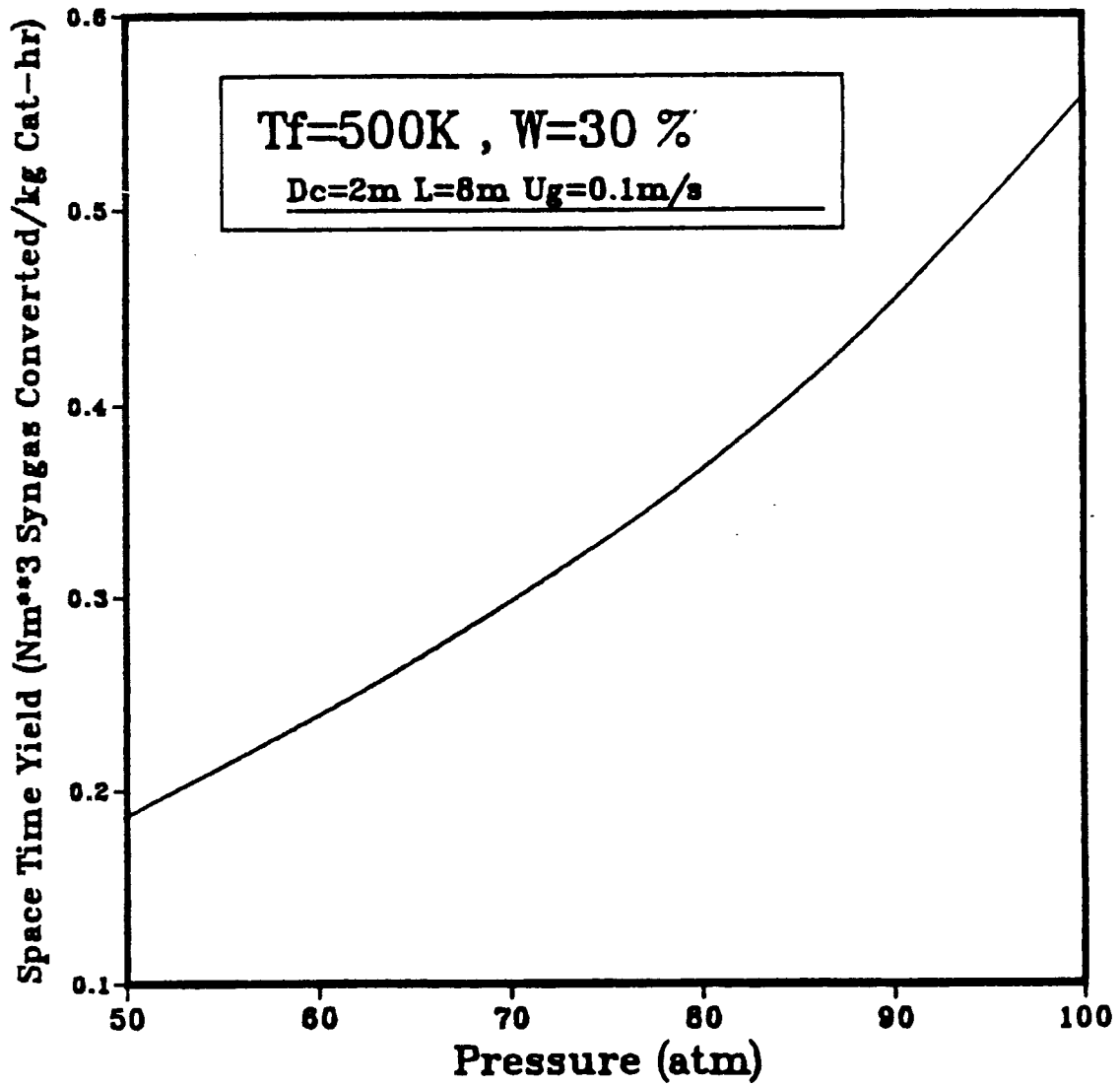


Figure I-C-29: Effect of pressure on STY

Comparison of the Performances of Fixed and Bubble Column Reactors for Methanol Synthesis

Based on the reactor performance computations a comparison has been made for two different reactor systems for methanol synthesis. Although a complete comparison should also involve economic considerations, a process design point of view has taken into account.

Fixed bed reactors are preferred because of ease in operation, absence of a second phase (liquid) but they have the drawback of temperature control. In fact a single bed is not possible to achieve the desired conversion and the reactor should be designed in a way that temperature control can be done. Operating conditions should also be carefully chosen to avoid equilibrium limitations. The reaction is found to be pore diffusion controlled hence the reaction rate is lowered significantly.

Slurry reactors are introduced to get a good solution for temperature control and to avoid pore diffusion by using a liquid and very fine catalyst particles respectively. However, the presence of a second phase (liquid) introduces another resistance in connection with mass transfer and solubility.

Generally speaking, each type of reactor has its own advantages and drawbacks. To have an idea about the performances of these units, the conversion and STY aspects are compared here. In the calculations the same feed conditions (composition, temperature, pressure) are used but to avoid equilibrium limitations, higher gas velocities and shorter bed lengths are used in fixed bed reactor. For slurry reactor, the catalyst loading was also varied.

In Fig. I-C-30 the conversion is plotted versus WHSV (weight hourly space velocity) for both reactors. It is clear that for the same space velocity (WHSV) slurry reactor can give higher conversions. Fig. I-C-31 shows the STY

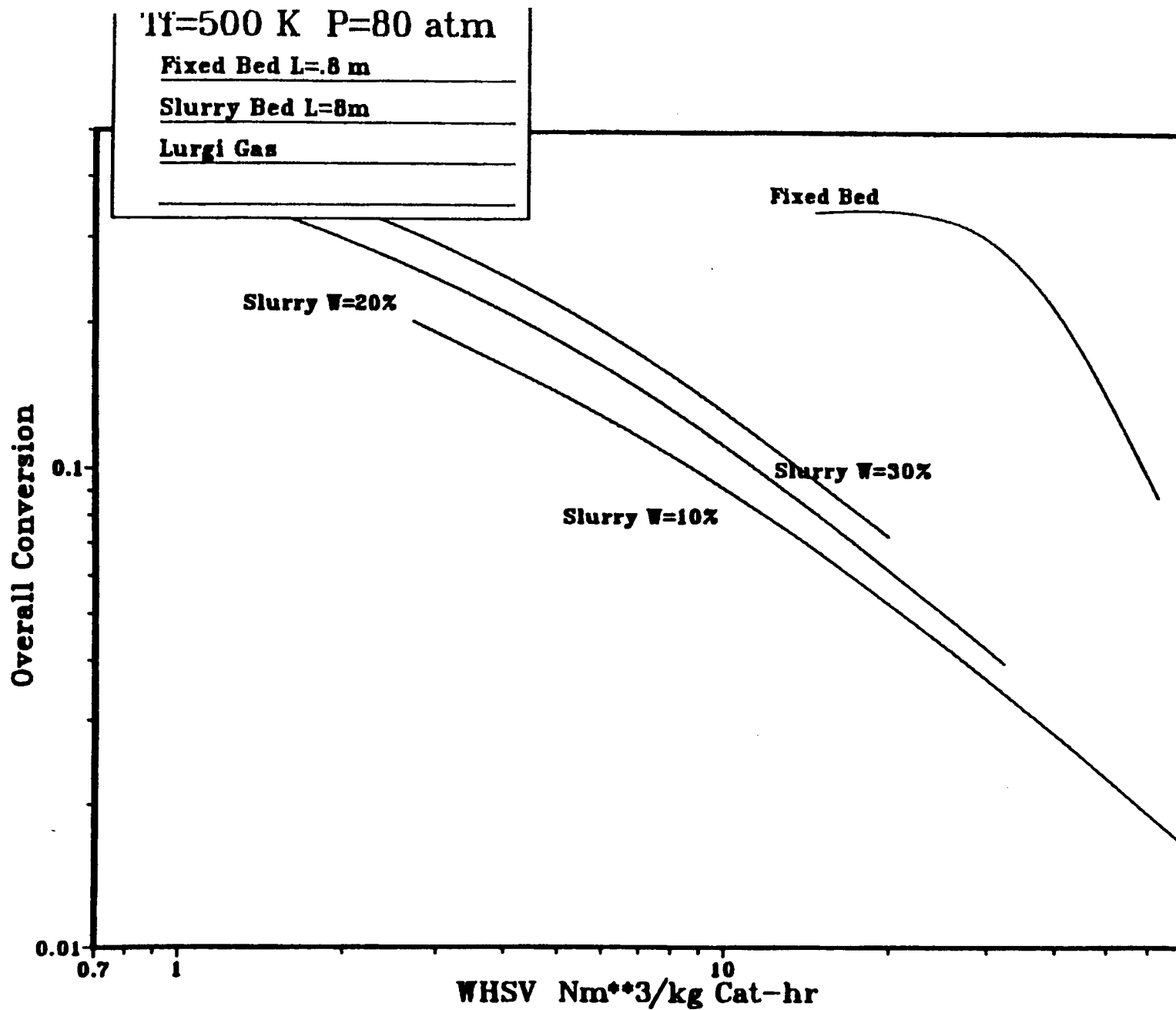


Figure I-C-30: Comparison of fixed and slurry bed reactors

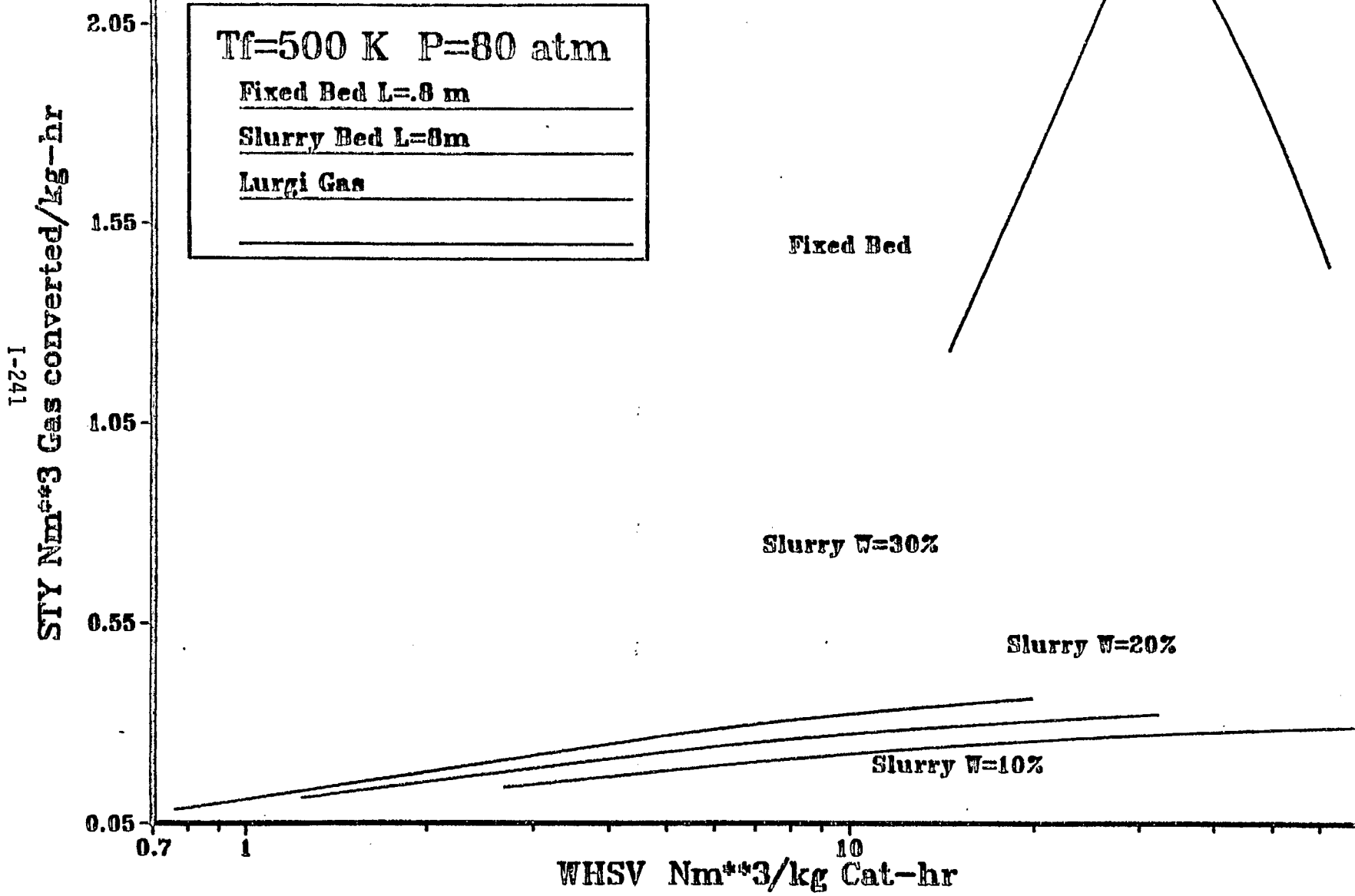


Figure I-C-31: Comparison of fixed and slurry bed reactors

of the reactors. Although STY for fixed bed reactors goes through a maxima, it always increases for slurry reactor. Obviously, Space Time Yield is much greater in fixed bed reactors but it may be lower for low space velocities.

Parameters Estimation for Fixed-Bed Reactor

1. Diffusivities:

Binary diffusivities are calculated by Fuller-Schetter-Giddings equation (Reid et al., 1977):

$$D_{ij} = \frac{10^{-7} T^{3/2} (1/M_i + 1/M_j)^{1/2}}{P (v_i^{1/3} + v_j^{1/3})^2} \quad \text{m}^2/\text{s}$$

The units are

T = Temperature, K

v_i = molal volume, cm^3/gmol

P = pressure, atm

The values of v_i and M_i (molecular weight) for methanol synthesis mixture are listed above

Component	M_i	v_i (cm^3/gmol)
CO	28	18.9
CO ₂	44	26.9
H ₂	2	7.07
CH ₃ OH	32	29.9
H ₂ O	18	12.7
N ₂	28	17.9
CH ₄	16	24.42

Gas mixtures diffusivities are calculated by the method of Wilke (Wilke and Lee, 1975):

$$D_{i,m} = \frac{1 - y_i}{\sum_{j=1}^n \frac{y_j}{D_{ij}}}$$

For the effective diffusivities in catalyst pores, the parallel pore model of the catalyst structure is assumed and the contribution of Knudsen diffusivities is neglected

$$D_{i,m}^e = D_{i,m} \left(\frac{\epsilon}{\tau} \right)$$

2. Viscosities:

Method of corresponding states is used to calculate the gas viscosities (Reid et al., 1977)

$$\mu_i = (1.9 T_{r,i} - 0.29) 10^{-7} z_{c,i}^{2/3} / \zeta_i \frac{\text{kg}}{\text{m-s}}$$

$$\zeta_i = T_{c,i}^{1/6} / (M_i^{1/2} P_{c,i}^{2/3})$$

$$T_{r,i} = T / T_{c,i}$$

Viscosity of the methanol synthesis gas mixture is calculated by Wilke's equation (Reid et al., 1977).

$$\mu_{\text{mix}} = \frac{\sum_{i=1}^n \frac{y_i M_i}{\sum_{j=1}^n y_j \phi_{ij}}}{\sum_{i=1}^n \frac{y_i M_i}{\sum_{j=1}^n y_j \phi_{ij}}}$$

where

$$\phi_{ij} = \frac{1}{\sqrt{8}} \left(1 + \frac{M_i}{M_j}\right)^{-1/2} \left[1 + \left(\frac{M_j}{M_i}\right)^{1/2} \left(\frac{\mu_i}{\mu_j}\right)^{1/4}\right]^2$$

The parameters involved in the calculations are as follows:

Component	M_i	T_c (K)	P_c (atm)	Z_c
CO	28	132.9	35.4	0.295
CO ₂	44	304.2	72.8	0.274
H ₂	2	33.2	12.8	0.305
CH ₃ OH	32	512.6	79.9	0.224
H ₂ O	18	647.3	217.6	0.229
N ₂	28	126.2	33.5	0.290
CH ₄	16	190.6	45.4	0.228

3. Heat Capacities:

Heat capacities are taken from the reference books in the form of

$$C_{p,i} = a_i + b_i T + c_i T^2 + d_i T^3 \quad \text{kJ/kmol.K, } T: \text{ }^\circ\text{C}$$

The values of a_i , b_i , c_i , d_i are as follows (Himmelblau, 1982):

Component	a	$b \times 10^2$	$c \times 10^5$	$d \times 10^9$
CO	28.95	.411	.3548	-2.22
CO ₂	36.11	4.233	-2.887	7.465
H ₂	28.84	0.00765	.3288	-.8698
CH ₃ OH	42.93	8.301	-1.89	-8.03
H ₂ O	33.46	.688	.760	-3.593

N ₂	29.0	.2199	.5723	-2.871
CH ₄	34.33	5.711	.3363	11.0092

Heat capacity of the methanol gas mixture is calculated by a simple mixing rule:

$$C_{p,m} = \sum C_{p,i} y_i$$

The mass heat capacity of the mixture is calculated by

$$C_{p,m} \text{ (mass)} = \sum C_{p,i} y_i / M_i : \text{kJ/kg-K}$$

4. Thermal Conductivities:

Thermal conductivity of each species is estimated by Bromley's Method (Reid et al., 1977).

The equations used are:

$$\text{For monatomic gases } \frac{\lambda M}{\mu} = 2.5 C_v$$

$$\text{For linear molecules } \frac{\lambda M}{\mu} = 1.30 C_v + 3.50 - 0.70/T_r$$

$$\text{For nonlinear molecules } \frac{\lambda M}{\mu} = 1.30 C_v + 3.66 - 0.3 C_{ir} - \frac{0.69}{T_r} - 3 \alpha$$

where λ = thermal conductivity, cal/cm-s-k

μ = viscosity, P

C_v = heat capacity at constant volume, cal/gmol-K

M = molecular weight

T_r = reduced temperature, T/T_c

α = collision interaction coefficient

$$\alpha = 3.0 \rho_b (\Delta S_{vb} - 8.75 - r \ln T_6)$$

ρ_b = molar density at boiling point, gmol/cm³

$\Delta S_{vb} = \Delta H_{vb}/T_b$: molar entropy change of vaporization cal/gmol-K

R = ideal gas constant, 1.987 cal/gmol-K

T_b = boiling point, K

C_{ir} = Internal-rotation heat capacity, cal/gmol-K

Numerical values of x_i are calculated at constant temperature of 500 K and assumed constant.

Carbon Monoxide (CO): Linear Molecule:

T_c = 132.9 K

C_p = 7.1239 cal/gmol-K

C_v = $C_p - 1.987$

T_b = 81.7 K

μ = $3.84 \cdot 10^4$ p

M = 28

gives $\lambda = 1.59 \cdot 10^{-4}$ kJ/m-s-K

Carbon Dioxide (CO₂): Linear Molecule:

T_c = 304.2 K

C_p = 10.595 cal/gmol/K

T_b = 194.7 K

μ = $2.995 \cdot 10^{-4}$ p

M = 44

gives $\lambda = 1.776 \cdot 10^{-4}$ kJ/m-s-K

Hydrogen (H₂): Linear Molecule:

$$T_c = 33.2 \text{ K}$$

$$C_p = 6.994 \text{ cal/gmol/K}$$

$$T_b = 20.4 \text{ K}$$

$$\mu = 2.698 \cdot 10^{-4} \text{ P}$$

$$M = 2$$

$$\text{gives } \lambda = 5.551 \cdot 10^{-5} \text{ kJ/m-s-K}$$

Methanol (CH₃OH): Nonlinear Molecule:

$$T_c = 512.6 \text{ K}$$

$$C_p = 14.215 \text{ cal/gmol-K}$$

$$T_b = 337.8 \text{ K}$$

$$\mu = 1.572 \cdot 10^{-4} \text{ P}$$

$$M = 32$$

$$\Delta H_{vb} = 8426 \text{ cal/gmol}$$

$$\rho = 0.791 \text{ gmol/cm}^3$$

$$\Delta S_{vb} = 24.94 \text{ cal/gmol-K } \alpha = 0.343$$

$$C_{ir} = 1.20$$

$$\text{gives } \lambda = 3.58 \cdot 10^{-6} \text{ kJ/m-s-K}$$

Water (H₂O): Nonlinear Molecule:

$$T_c = 647.3 \text{ K}$$

$$C_p = 8.454 \text{ cal/gmol-K}$$

$$T_b = 373.2 \text{ K}$$

$$\mu = 1.642 \cdot 10^{-4} \text{ P}$$

$$M = 18$$

$$\Delta H_{vb} = 9717 \text{ cal/gmol}$$

$$\rho = 0.998 \text{ gmol/cm}^3$$

$$\Delta S_{vb} = 26.04 \text{ cal/gmol-K} \quad \alpha = 0.90$$

$$C_{ir} = 1.20$$

gives $\lambda = 4.165 \cdot 10^{-6} \text{ kJ/m-s-K}$

Nitrogen (N_2): Linear Molecule:

$$T_c = 126.2 \text{ k}$$

$$C_p = 7.07 \text{ cal/gmol-K}$$

$$T_b = 77.4$$

$$\mu = 4.05 \cdot 10^{-4} \text{ P}$$

$$M = 28$$

gives $\lambda = 1.67 \cdot 10^{-4} \text{ kJ/m-s-K}$

Mathane (CH_4): Nonlinear molecule:

$$T_c = 190.6 \text{ K}$$

$$C_p = 11.200 \text{ cal/gmol-K}$$

$$T_p = 111.7 \text{ K}$$

$$\mu = 2.669 \cdot 10^{-4} \text{ P}$$

$$M = 16$$

$$\Delta H_{vb} = 1955 \text{ cal/gmol}$$

$$\rho = 0.425 \text{ gmol/cm}$$

$$\Delta S_{vb} = 17.50 \text{ cal/gmol-K} \quad \alpha = -0.049$$

$$C_{ir} = 2.12$$

gives

$$\lambda = 1.045 \cdot 10^{-5} \text{ kJ/m-s-K}$$

Thermal conductivity of the methanol synthesis gas mixture is calculated by Linsay-Bromley equation (Reid et al., 1977):

$$\lambda_m = \frac{\sum_{i=1}^n y_i \lambda_i}{\sum_{i=1}^n y_i A_{ij}}$$

where

$$A_{ij} = \frac{1}{4} \left\{ 1 + \left[\frac{M_i}{M_j} \left(\frac{M_j}{M_i} \right)^{3/4} \frac{T + S_i}{T + S_j} \right]^{1/2} \right\}^2 \frac{T + S_{ij}}{T + S_i}$$

where

μ_i = pure gas viscosity

T = absolute temperature

S = Sutherland constant

$S_i = 1.5 T_{bi}$ (boiling point)

and S_{ij} = interaction Sutherland constant

$$S_{ij} = S_{ji} = C_s (S_i S_j)^{1/2}$$

the S values are

Component	S_i (K)
CO	122.6
CO ₂	292.1
H ₂	30.6
CH ₃ OH	506.7
H ₂ O	116.1
N ₂	167.6
H ₂ O	559.8

5. Mass Transfer Coefficients:

The following correlation is used for $(k_g)_i$ values (Smith, 1981):

$$J_D = \frac{0.458}{\epsilon_B} \left(\frac{d G}{\mu} \right)^{-0.407} = J_H$$

$$= \frac{(k_g)_i}{U} \left(\frac{\mu}{\rho D_i} \right)^{2/3}$$

where

$$G = U \rho \quad \rho = \frac{PM}{RT}$$

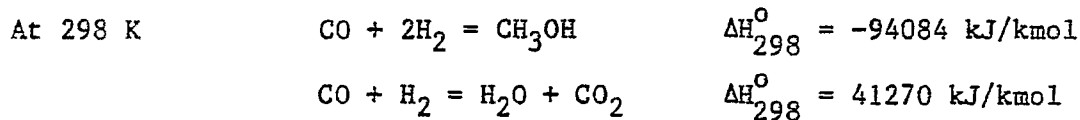
$$\bar{M} = \sum M_i y_i$$

6. Heat Transfer Coefficient:

Taking $J_D = J_H$, h values are calculated by

$$J_H = \frac{h}{C_p G} \left(\frac{C_p \mu}{\lambda} \right)^{2/3}$$

7. Reaction Enthalpies:



For any temperature using C_p values,

$$\Delta H_T^{\circ} = \Delta H_{298}^{\circ} + \int_{298}^T \Delta C_p dT$$

where

$\Delta = \text{products} - \text{reactants}$

and hence C_p values are expressed as

$$C_p = a + bT + cT^2 + dT^3$$

we can get

$$\Delta H_T^{\circ} = \Delta H_{298}^{\circ} + \Delta a (t - 25) + \frac{\Delta b}{2} (t^2 - 25^2) + \frac{\Delta c}{3} (t^3 - 25^3)$$

$$+ \frac{\Delta d}{4} (t^4 - 2.5^4)$$

for C_p values $^{\circ}\text{C}$ is used.

8. Catalyst Properties:

The following properties are reported in the literature for Cu/ZnO/Al₂O₃ catalyst (Villa et al., 1985):

Thermal Conductivity	$\lambda_e = 4.18 \cdot 10^{-3} \text{ kJ/m-s-K}$
Density	$\rho_p = 1980 \text{ kg/m}^3$
Porosity	$\epsilon_p = 0.3$
Tortousity	$\tau = 7$

9. Reaction Kinetics:

Several kinetic studies have been reported in the literature for different catalysts. Although this work concerns with low pressure synthesis where Cu-based catalysts are applied, most of the kinetic rate expressions are presented here. In the studies the main emphasis is given to the main reaction, i.e. methanol formation reaction (reaction 1) and shift reaction (reaction 2) is assumed to be at equilibrium. In some investigations reaction 3 is considered instead of reaction 1.

The kinetic data for gas phase studies can, in principle, be applied to liquid phase synthesis but it is desirable to use a rate expression obtained in actual three phase system. Studies for the latter case are very scarce and only one detailed expression is available.

a) The kinetics of the methanol-synthesis reaction, on either a ZnO-Cr₂O₃ (ratio of 89:11) catalyst or a ZnO-CuO/Cr₂O₃ (ratio of 50:25:25) catalyst were studied by Natta (1955) and his coworkers in a carefully designed laboratory apparatus under commercial synthesis condition. They developed a kinetic expression for the temperature range of about 330 to 390°C

that is used as a basis for design of commercial high pressure methanol synthesis reactors.

Natta's kinetic expression is

$$r_1 = \frac{f_{\text{CO}} f_{\text{H}_2}^2 - f_{\text{CH}_3\text{OH}}/K_{\text{eq},1}}{(A + B f_{\text{CO}} + C f_{\text{H}_2} + D f_{\text{CH}_3\text{OH}})^3}$$

where driving forces are expressed in terms of fugacities and A, B, C, and D are parameters that are a function of temperature. This equation is derivable in terms of Langmuir-Hinshelwood kinetics in which the surface reaction is taken to be a trimolecular process between two molecules of adsorbed H₂ and one of CO.

The constants, B, C and D are proportional to the adsorption equilibrium constants K_{CO}, K_{H₂} and K_{CH₃OH}, respectively, in the Langmuir-Hinshelwood formulation and, in accordance with theory, decrease with decreased temperature. The values for these constants are given by Natta in graphical forms. Some investigators have fitted those by the following (Stiles, 1977):

$$A = 216.07 \cdot 10^{[3.50192 - 1.2921 \log_{10}(0.1T - 50)]}$$

$$B = A [10^{(-9.911 - 5180/T)}]$$

$$C = A [10^{(-13.942 - 7230/T)}]$$

$$D = A [10^{(-11.901 - 8780/T)}]$$

and the rate is in kmol/hr-kg.

b) Cappelli and Dente (1965) modified the above expressions for a ZnO-Cr₂O₃ catalyst to include a term for CO₂. By comparison of the results at their calculations with the performance at an industrial reactor, they

conclude that the water gas shift reaction, (reaction 2) goes rapidly to equilibrium. The rate expression for methanol formation has been assumed as

$$r_1 = \frac{f_{\text{CO}} f_{\text{H}_2}^2 - f_{\text{CH}_3\text{OH}}/K_{\text{eq},1}}{A^3 (1 + Bf_{\text{CO}} + Cf_{\text{H}_2} + D f_{\text{CH}_3\text{OH}} + E f_{\text{CO}_2})^3} \quad ; \frac{\text{k mol}}{\text{hr-kg}}$$

where the following values have been taken for A, B, C, D, E:

$$\begin{aligned} A &= \frac{2.78 \cdot 10^5}{(5A)^{1/3}} \exp(-4167/T) \\ B &= 1.33 \cdot 10^{-10} \exp(12,003/T) \\ C &= 4.72 \cdot 10^{-14} \exp(15,350/T) \\ D &= 5.05 \cdot 10^{-14} \exp(15,727/T) \\ E &= 3.33 \cdot 10^{-10} \exp(12,003/T) \end{aligned}$$

with

$$SA = 70 \text{ m}^2/\text{g}$$

Beside these two rate equations for high pressure synthesis, studies have been reported in the literature concerning the Cu-based low pressure synthesis catalysts:

c) A CuO/ZnO catalyst (BASF) has been applied in the kinetic study of methanol synthesis by Schermuly and Luft (1978). A rate expression similar to these derived by Natta and Cappelli and Dente has been presented:

$$r_1 = \frac{f_{\text{CO}} f_{\text{H}_2}^2 - f_{\text{CH}_3\text{OH}}/K_{\text{eq},1}}{(A + B f_{\text{CO}} + C f_{\text{H}_2} + D f_{\text{CH}_3\text{OH}} + E f_{\text{CO}_2})^2} \quad \frac{\text{kmol}}{\text{hr-kg}}$$

with

$$\begin{aligned} A &= 6.33 \cdot 10^{14} \exp(-15,432/T) \\ B &= 2.28 \cdot 10^{-3} \exp(4739/T) \end{aligned}$$

$$C = 2.12 \cdot 10^{-6} \exp(7818/T)$$

$$D = 8.14 \exp(-467.1/T)$$

$$E = 2.03 \cdot 10^{-11} \exp(43,952/T)$$

The shift reaction (reaction 2) was again assumed to be at equilibrium

d) For Cu/Zn/Cr₂O₃ catalyst (United catalyst T-2370) Berty et al. (1981) obtained

$$r_1 = k_1 \left(C_{H_2} - \frac{C_{MEOH}}{K_{eq,1} C_{H_2} C_{CO}} \right) \quad ; \quad \frac{\text{kmol}}{\text{hr-kg}}$$

and for the shift reaction

$$r_2 = k_2 \left(C_{H_2} - \frac{C_{CO} C_{H_2O}}{K_{eq,2} C_{CO_2}} \right); \quad \frac{\text{kmol}}{\text{hr-kg}}$$

For rate constants the values reported are:

$$k_1 = 14092 \exp(-9386/T)$$

$$k_2 = 42.804 \exp(-5068.4/T)$$

The same equations were found to be applicable for liquid phase synthesis (Berty et al. 1983). The only difference is the exponent in k_1 should be (-7489/T) for the latter case.

e) Klier et al. (1982) have investigated the kinetics of low pressure synthesis for a Cu/Zn/Al₂O₃ catalyst, with special attention to the role of CO₂. They have considered reaction 1 and 3 as independent reactions and proposed the following rate expressions:

$$r_1 = k_1 \frac{K(P_{CO_2}/P_{CO})^3}{[1+K(P_{CO_2}/P_{CO})]^3} \frac{K_{CO} K_{H_2}^2 (P_{CO} P_{H_2})^2 - P_{MeOH}/D_{eq,1}}{(1+K_{CO} P_{CO} + K_{CO_2} P_{CO_2} + K_{H_2} P_{H_2})^3}; \quad \frac{\text{kmol}}{\text{kg-sec}}$$

and

$$r_3 = k_3 \left(P_{CO} - \frac{1}{K_{eq,3}} \frac{P_{MeOH} P_{H_2O}}{P_{H_2}^3} \right); \quad \frac{\text{kmol}}{\text{kg-sec}}$$

The rate for reaction 2 can be calculated as

$$r_2 = r_3 - r_1$$

The numerical values for constants are as follows:

$$\begin{aligned} k_1 &= 1.209 \exp(-4,142/T) \\ K &= 1.17 \cdot 10^{-3} \exp(9,889/T) \\ K_{CO} &= 1.61 \cdot 10^{-8} \exp(10,222/T) \\ K_{H_2} &= 4.44 \cdot 10^{-6} \exp(6,438/T) \\ K_{CO_2} &= 3.03 \cdot 10^{-13} \exp(16,222/T) \\ k_3 &= 5.35 \cdot 10^{-3} \exp(-5.677/T) \end{aligned}$$

f) Villa et al. (1985) have reported a kinetic study of methanol synthesis reaction over a commercial Cu/ZnO/Al₂O₃ catalyst at temperatures, pressures and gas compositions typical of industrial operation. Both reactions 1 and 2 were considered. The rate equations are:

$$r_1 = \frac{(f_{CO} f_{H_2}^2 - f_{CH_3OH}/K_{eq,1})}{(C_1 + C_2 f_{CO} + C_3 f_{CO_2} + C_4 f_{H_2})^3}; \quad \frac{\text{kmol}}{\text{kg-min}}$$

$$r_2 = \frac{f_{CO} f_{H_2} - f_{CO} f_{H_2O}/K_{eq,2}}{C_6}; \quad \frac{\text{kmol}}{\text{kg-min}}$$

The following parameter estimates were obtained

$$C_1 = 1.881 \cdot 10^{-3} \exp(4883/T)$$

$$C_2 = 4.21 \cdot 10^{34} \exp(-39060/T)$$

$$C_3 = 8.296 \cdot 10^{-13} \exp(15948/T)$$

$$C_4 = 4.036 \cdot 10^{-7} \exp(8229/T)$$

$$C_6 = 1.581 \cdot 10^{-6} \exp(9380/T)$$

10. Equilibrium Constants:

The equilibrium constants $K_{eq,1}$, $K_{eq,2}$, $K_{eq,3}$ are defined by their relations to the equilibrium partial pressures

$$K_{eq,1} = \left(\frac{P_{CH_3OH}}{P_{H_2}^2 P_{CO}} \right)_{eq}$$

$$K_{eq,2} = \left(\frac{P_{CO} P_{H_2O}}{P_{CO} P_{H_2}} \right)_{eq}$$

$$K_{eq,3} = \left(\frac{P_{CH_3OH} P_{H_2O}}{P_{H_2}^3 P_{CO_2}} \right)_{eq}$$

or

$$K_{eq,2} = K_{eq,1} \times K_{eq,3}$$

They are related to the true equilibrium constants $K_{p,1}$ and $K_{p,3}$ ($K_{p,2}$ or $K_{eq,2}$ one related by the last relationship) at a total pressure of one atmosphere through the fugacity ratios $K_{\gamma,1}$ and $K_{\gamma,3}$

$$K_{eq,1} = K_{p,1}/K_{\gamma,1}; K_{eq,3} = K_{p,3}/K_{\gamma,3}$$

The K_p are functions of temperature only, while the K_γ are functions of both temperature and pressure. Their P, T dependencies of K_p and K_γ were taken from Stiles (1977) in the form

$$K_{p,1} = 3.27 \cdot 10^{-13} \exp(11678/T)$$

$$K_{\gamma,1} = 1 - A_1 P$$

$$A_1 = 1.95 \cdot 10^{-4} \exp(1703/T)$$

$$K_{p,3} = 3.826 \cdot 15^{11} \exp(6851/T)$$

$$K_{\gamma,3} = (1 - A_1 P) (1 - A_2 P)$$

$$A_2 = 4.24 \cdot 10^{-4} \exp(1107/T)$$

For liquid phase $K_{\gamma,1}$ and $K_{\gamma,3}$ are taken unity.

11. Fugacities:

Fugacity coefficients of the components were calculated by generalized expressions presented in terms of reduced temperature and pressure (Ferraris and Donati, 1971):

$$\ln \phi_1 = \frac{1}{0.0833} \left\{ \left(\frac{1.01961 \cdot 10^{-2}}{T_r} - \frac{2.142 \cdot 10^{-2}}{T_r^2} - \frac{3.2548 \cdot 10^{-2}}{T_r^4} \right) Pr + \right.$$

$$\begin{aligned}
& + \left(\frac{1.8496 \cdot 10^{-3}}{T_r^3} - \frac{2.1511 \cdot 10^{-3}}{T_r^5} + \frac{0.91445 \cdot 10^{-2}}{T_r^7} \right) P_r^2 + \\
& + \left(\frac{-0.4172 \cdot 10^{-4}}{T_r^3} + \frac{1.5469 \cdot 10^{-4}}{T_r^5} - \frac{0.5191 \cdot 10^{-4}}{T_r^7} \right) P_r^3 + \\
& + \left(\frac{0.42548 \cdot 10^{-6}}{T_r^3} - \frac{0.28052 \cdot 10^{-5}}{T_r^5} - \frac{0.82075 \cdot 10^{-5}}{T_r^7} \right) P_r^4 \}
\end{aligned}$$

and the fugacities are calculated as

$$f_i = \phi_i y_i P$$

Parameter Estimation for Slurry Bed Reactor

1. Physical Properties of Liquid Phase:

The following quantities are used for Witco-40 ($C_{18}H_{38}$).

Density (Reid et al., 1977)

$$\rho_L = 620 \text{ kg/m}^3 \text{ and assumed constant.}$$

Viscosity (Reid et al., 1977)

$$\mu = 8.8778 \cdot 10^{-6} \cdot 10^{777.4/T} \text{ kg/m-s and } T \text{ in K.}$$

Surface Tension (Berty et al., 1981)

$$\sigma = 0.016 \text{ N/m and assumed constant.}$$

2. Heat Capacity:

Estimated for $C_{18}H_{38}$ by using the group contribution method of Luria and Benson (Reid et al., 1977, page 154).

<u>Number</u>	<u>Group</u>	<u>A</u>	<u>B</u>	<u>C</u>	<u>D</u>
2	C-(C)(H) ₃	8.459	$2.113 \cdot 10^{-3}$	$-5.605 \cdot 10^{-5}$	$1.723 \cdot 10^{-7}$
16	C-(C) ₂ (H) ₂	-1.383	$7.049 \cdot 10^{-2}$	$-2.063 \cdot 10^{-4}$	$2.269 \cdot 10^{-7}$

$$C_p = A + BT + CT^2 + DT^3 \text{ cal/gmol-K}$$

at 500K and for a molecular weight of 250 kg/kmol we get:

$$C_p = 18549 \frac{\text{cal}}{\text{gmol-K}} \text{ or } C_p = 31.06 \frac{\text{kJ}}{\text{kg-K}}$$

3. Diffusivities of the Gases in Liquid Phase:

Diffusivities are estimated by Wilke-Chang equation (Reid et al., 1977, page 567):

$$D_{i,B} = 1.173 \cdot 10^{-16} \frac{(\phi M_B)^{1/2} T}{\mu_B V_i^{0.6}}$$

where $\phi = 1$ association factor

$M_B = 250$ molecular weight for solvent

$\mu =$ viscosity at solvent, kg/m-s

$V_i =$ molar volume of solute i at its normal boiling temperature,
 m^3/kmol

The V_i values are:

<u>Component</u>	<u>$V_i \text{ m}^3/\text{kmol}$</u>
CO	0.0307
CO ₂	0.0340
H ₂	0.0143
CH ₃ OH	0.0259
H ₂ O	0.0189

4. Solubilities:

Solubility and liquid-vapor equilibrium data of the species reported in the literature (Berty et al., 1981) are expressed as Henry's constants:

$$H_i = A_i e^{-B_i/T} \text{ atm-m}^3/\text{kmol}, T \text{ in K.}$$

where the constants are as follows:

<u>Component</u>	<u>A</u>	<u>B</u>
CO	20.73	1015.5
CO ₂	618.39	-849.1
H ₂	11.25	1289.5
CH ₃ OH	352249	-4307
H ₂ O	993095	-4890

For the pressure and temperature range of the conditions used, these values are found to be applicable for the solubilities of the gases in Witco-40 medium.

5. Properties of suspension:

Density

$$\bar{\rho} = v_{\text{cat}} \rho_{\text{cat}} + (1-v_{\text{cat}}) \rho_L \text{ kg/m}^3$$

where

$$v_{\text{cat}} = \frac{\rho_L W_{\text{cat}}}{\rho_{\text{cat}} - W_{\text{cat}}(\rho_{\text{cat}} - \rho_L)}$$

and

$$W_{\text{cat}} = M_{\text{cat}}/M_{\text{sus}}, \text{ i.e., weight fraction of catalyst in suspension.}$$

Viscosity

No correlation has been reported in the literature for the slurry viscosities of Witco-40 suspensions. Therefore, the correlation by Deckwer et al., (1980) is assumed to be applicable.

$$\bar{\mu} = \mu_L (1 + 4.5 V_{cat}) \text{ kg/m-s}$$

Heat Capacity

$$\bar{C}_p = W_{cat} C_{p,cat} + (1 - W_{cat}) C_{p,L}$$

6. Mass Transfer and Hydrodynamic Properties:

Gas Holdup (Akita-Yoshida, 1973)

$$\frac{\epsilon_G}{(1 - \epsilon_G)^4} = 0.2 \left(\frac{g D_c^2 \rho_L}{\sigma} \right)^{1/8} \left(\frac{g D_c^3}{v_L^2} \right)^{1/12} \left(\frac{U_G}{\sqrt{g D_c}} \right)$$

The value of gas holdup (ϵ_G) is assumed to be unaffected by the presence of solid.

Mass Transfer Coefficient (Akita-Yoshida, 1974)

$$(k_{La})_i \frac{D_c^2}{D_i} = 0.6 \epsilon_G^{1.1} \left(\frac{v_L}{D_i} \right)^{0.5} \left(\frac{g D_c^2 \rho_L}{\sigma} \right)^{0.62} \left(\frac{g D_c}{v_L^2} \right)^{0.31} \text{ m}^2/\text{s}$$

7. Dispersion Coefficients:

Liquid Phase (Shah and Deckwer, 1985)

$$D_L = 0.768 U_G^{0.32} D_c^{1.34} \text{ m}^2/\text{s}$$

Heat Dispersion coefficient in the liquid

$$\lambda_{ax} = D_L \bar{\rho} \bar{C}_p \text{ kJ/m-s-K}$$

8. Solid Phase Dispersion and Sedimentation (Kato et al., 1972):

Dispersion coefficient

$$Bo_C = \frac{U_G D_c}{D_s} = \frac{13 Fr}{1 + 8 Fr^{0.85}}$$

with

$$Fr = U_G \sqrt{g D_c}$$

Settling velocity in particle swarm

$$U_{ss} = 1.2 U_{st} \left(\frac{U_G}{U_{st}} \right)^{0.25} \left(\frac{1 - v_{cat}}{1 - v_{cat}^*} \right)^{2.5}$$

where

$$v_{cat}^* \text{ is } v_{cat} \text{ at } C_{cat} = 0.1 \text{ g/cm}^3$$

The settling velocity of a single particle, U_{st} , is calculated from

$$Re = Ar/18 \text{ if } Re < 0.5$$

$$Re = (Ar/13.9)^{0.7} \text{ if } Re > 0.5$$

where

$$Ar = \frac{\rho_L (\rho_{cat} - \rho_L) g}{\mu_L^2} d_p^3$$

$$Re = \frac{U_{st} d_p}{\nu_L}$$

Nomenclature

a_v	: Gas-solid interfacial area, m^{-1}
Be	: Dimensionless energy group, eq. 83c
Bo_L	: Liquid phase Bodenstein number, eq. 85b
Bo_L^*	: Liquid phase Bodenstein number, eq. 88b
Bo_s	: Solid phase Bodenstein number, eq. 88a
C_{ij}, C^g	: Gas phase concentrations, $kmol/m^3$
C_{ig}^*	: Equilibrium concentration in liquid phase, $kmol/m^3$
C^s	: Solid phase concentration, $kmol/m^3$
C_{il}	: Liquid phase concentration, $kmol/m^3$
C_T, C_G	: Total gas concentration, $kmol/m^3$
C_{cat}	: Catalyst concentration, kg/m^3
C_P	: Heat capacity, $kJ/kg-K$
D	: Diffusion coefficient, m^2/s
D_G	: Gas phase dispersion coefficient, m^2/s
dp	: Particle diameter, m
D_s	: Solid phase dispersion coefficient, m^2/s
Da	: Damkoehler number, eq. 85f
F	: Total molal flow rate (slurry), $kmol/s$
H	: Henry's constant, $atm-m^3/kmol$
h	: Heat transfer coefficient, kJ/m^2-s-K
ΔH_R	: Reaction enthalpy, $kJ/kmol$
k	: Rate constant, $m^3/kg-sa$
k_g	: Mass transfer coefficient, m/s
$k_L a$: Volumetric mass transfer coefficient, s
L	: Length, m
N	: Superficial molal flow rate (fixed bed), $kmol/m^2-s$

Nu : Nusselt number, eq. 47
 P : Pressure, atm
 Pe : Peclet number for heat transfer, eq. 83b
 q : flow rate ratio, slurry/gas
 r : Radial coordinate, m
 r : Reaction rate, kmol/kg-s
 R : Particle radius, m
 R : Universal gas constant
 Re : Reynolds number
 Sh : Sherwood number, eq. 47
 St_G : Stanton number in gas phase, eq. 83d
 St_L : Stanton number in liquid phase, eq. 85a
 T : Temperature, K
 T^G : Gas phase temperature, K
 T^S : Solid phase temperature, K
 U, U_G : Superficial gas flow rate, m/s
 U_L : Superficial liquid flow rate, m/s
 U_{SS} : Settling velocity of catalyst particles in swarm, m/s
 x : Axial coordinate, m
 x : Dimensionless liquid phase concentration, eq. 83f
 X : Conversion
 y : Mole fraction in gas phase
 z : Dimensionless axial coordinate

 Greek
 α : Dimensionless parameter, eq. 35
 α₁ : Parameter, eq. 27
 β : Parameter, eq. 27

Γ : Dimensionless heat of reaction, eqs. 36 and 37
 ϵ_B : Bed void fraction
 ϵ_G : Gas holdup
 ϵ_L : Liquid holdup
 ϵ_P : Particle porosity
 ζ : Dimensionless radial coordinate, r/R
 ϕ : Dimensionless rate, eqs. 31, 32 and 85e
 η : Effectiveness factor, eqs. 81 and 82
 λ : Thermal conductivity, kJ/m-s-K
 λ_{ax} : Heat dispersion coefficient, kJ/m-s-K
 ρ : Density, kg/m^3
 ρ_P : Particle density, kg/m^3
 θ : Dimensionless temperature, eqs. 34 and 83e
 ψ : Dimensionless catalyst concentration, eq. 85d
 ψ : Dimensionless reaction rate, eqs. 73 and 74
 ν : Stoichiometric coefficient

Subscript

e : Effective
 f : Feed
 g : Gas
 i : i th component
 k : k th reaction
 l : Liquid
 m : Mixture
 o : inlet
 s : solid

References:

- Akita, K., and Yoshida, F., "Gas Holdup and Volumetric Mass Transfer Coefficient in Bubble Columns", *Ind. Eng. Chem. Proc. Des. Dev.*, 12, 76 (1973).
- Akita, K., and Yoshida, F., "Bubble Size, Interfacial Area, and Liquid Phase Mass Transfer Coefficients in Bubble Columns", *Ind. Eng. Chem. Proc. Des. Dev.*, 13, 84 (1974).
- Ascher, U., Christiansen, J., and Russel, R.D., "Algorithm 569 COLSYS: Collocation Software for Boundary-Value ODEs", *ACM Trans. Math. Softw.*, 7, 223 (1981).
- Bakemeier, H., Laurer, P.R., and Schroder, W., *Chem. Eng. Prog. Symp. Ser.* (No. 78) 66, 1 (1970).
- Berty, J.M., Lee, S., Sivagnanam, K., and Szeifert, F., "Diffusional Kinetics of Catalytic Vapor-Phase Reversible Reactions with Decreasing Total Number of Moles", *I. Chem. E. Symposium Series No. 87* (1981).
- Berty, J.M., Lee, S., Parekh, V., Gandhi, R., and Sivagnanam, K., "Diffusional Kinetics of Low Pressure Methanol Synthesis", *Proceedings of PACHEC 83*, Vol. II, 191 (1983).
- Bonnell, L.W., and Weimer, R.F., "Slurry Reactor Design for Methanol Production", paper presented at the 1984 AIChE J Annual Meeting, San Francisco, 25-30 Nov. (1984).
- Brainard, A., Shah, Y.T., Tierney, J., Wender, I., Albal, R., Bhattacharjee, S., Joseph, S., and Seshadri, K., "Coal Liquefaction-Investigation of Reactor Performance, Role of Catalysts, and PCT Properties", Technical Progress Report, DOE Contract No. DE-FG22-83PC60056, University of Pittsburgh (1984).
- Brown, D.M., and Greene, M.I., "Catalyst Performance in Liquid Phase Methanol Synthesis", Paper presented at AIChE J Meeting, Philadelphia, 19-22 Aug. (1984).
- Cappelli, A., and Dente, M., "Kinetics and Methanol Synthesis", *Chim. Ind. (Milan)*, 47, 1068 (1965).
- Cappelli, A., Collina, A., and Dente, M., "Mathematical Model for Simulating Behavior of Fauser-Montecatini Industrial Reactors for Methanol Synthesis", *Ind. Eng. Chem. Proc. Des. Dev.*, 11, 185 (1972).
- Chang, C.D., "Hydrocarbons from Methanol", Marcel Dekker, Inc., New York, NY (1983).
- Cova, D.R., *Ind. Eng. Chem. Proc. Des. Dev.*, 5, 21 (1966).
- Deckwer, W.-D., Lousi, Y., Zaidi, A., Ralek, M., "Hydrodynamic Properties of Fischer-Tropsch Slurry Process", *Ind. Eng. Chem. Proc. Des. Dev.*, 19, 699 (1980).

- Deckwer, W.-D., Nguyen-tien, K., Kelkar, B.G., and Shah, Y.T., "Applicability of Axial Dispersion Model to Analyze Mass Transfer Measurements in Bubble Columns", *AIChE J.* 29, 915 (1983).
- Ferraris, G.B., and Donati, G., "Analysis of the Kinetic Models for the Reaction of Synthesis of Methanol", *Ing. Chim. Ital.*, 7 (4), 53 (1971).
- Froment, G.F., "Fixed-Bed Catalytic Reactors Technological Fundamentals Design Aspects", *Chem. Eng. Techn.*, 46, 374 (1974).
- Froment, G.F., and Bischoff, K.B., "Chemical Reactor Analysis and Design", John Wiley and Sons, Inc. (1979).
- Himmelblau, D.M., "Basic Principles and Calculations in Chemical Engineering", Prentice-Hall, 4th Ed., N.J. (1982).
- Kato, Y., Nishiwaki, A., Takashi, F., and Tanaka, S., "The Behavior of Suspended Solid Particles and Liquid in Bubble Columns", *J. Chem. Eng. Japan*, 5 112 (1972).
- Klier, K., Chatkikavanij, V., Herman, R.G., and Simmons, G.W., "Catalytic Synthesis of Methanol from CO/H₂, IV. The Effects of Carbon Dioxide", *J. Catalysis* 74, 343 (1982).
- Kung, H.H., "Methanol Synthesis", *Catal. Rev. - Sci. Eng.*, 22, 235-259 (1980).
- Macnaughton, N.J., Pinto, A., and Rogerson, P.L., "Development of Methanol Technology for Future Fuel and Chemical Markets", *Energy Progress*, 4 (1) 232 (1984).
- Natta, G., "Catalysis (Emmet, P.H., Ed). Vol. VIII, Reinhold, New York, p. 349 (1955).
- Reid, R.C., Sherwood, T.K., and Prausnitz, J., "The Properties of Gases and Liquids", 3rd Ed., McGraw-Hill, New York (1977).
- Shah, Y.T., Kelkar, B.G., Godbole, S.P., and Deckwer, W.-D., "Design Parameters Estimation for Bubble Column Reactors", *AIChE J.* 28 (3), 353 (1982).
- Shah, Y.T., and Deckwer, W.-D., "Scale Up Aspects of Fluid-Fluid Reaction," *Scale-Up in Chemical Process Industries*, ed., R. Kobal and A. Bisio, John Wiley (to be published, 1985).
- Shermuly, O., Luft, G., "Low Pressure Synthesis of Metahnol in a Jet-Loop-Reactor," *Ger. Chem. Eng.* 1, 22 (1978).
- Sherwin, M., and Blum, D., "Liquid Phase Methanol," EPRI Report, EPRI AF-1291, Chem. Systems, Inc. (1977).
- Sherwin, M.B., and Frank, M.B., "Make Methanol by Three Phase Reaction," *Hydrocarbon Processing*, p. 122 (Nov. 1976).

Salth, J.M., "Chemical Engineering Kinetics," McGraw Hill Co., 3rd ed., New York (1981).

Stiles, A.B., "Methanol Past, Present, and Speculations on the Future," AIChE J. 23 (3), 362 (1977).

Villa, P., Forzatti, P., Ferraris, G.B., Garone, G., and Pasquon, I., "Synthesis of Alcohols from Carbon Oxides and Hydrogen. I. Kinetics of the Low-pressure Methanol Synthesis," Ind. Eng. Chem. Process Des. Dev. 24, 12 (1985).

Wilke, C.R., and Lee, C.Y., Ind. Eng. Chem. 47, 1253 (1965).